EUROPEAN SOUTHERN OBSERVATORY

Organisation Européene pour des Recherches Astronomiques dans l'Hémisphère Austral
Europäische Organisation für astronomische Forschung in der südlichen Hemisphäre

Chile: Casilla 19001, Santiago 19
Germany: Karl-Schwarzschild-Str. 2, D-85748 Garching b. München

LA SILLA INSTRUMENTATION

Wide Field Imager (WFI)

USER MANUAL

Doc. No. LSO-MAN-ESO-22100-00001

Issue 1.0.7

26 March, 2002

Prepared by: Dietrich Baade

Change Record

Issue/Rev.	Date	Section/Parag. affected	Reason/Initiation/Documents/Remarks
1.0	19/01/99	All	1st release
1.0.1	15/02/99	A.2, A.3	more filter transmission data
1.0.2	23/02/99	A.2, A.3	more filter transmission data
1.0.3	03/03/99	2.5.1.1	description of mosaic geometry
1.0.4	25/05/99	2.2.2	updated filter tables
		2.3	added figure with grism geometry
		2.8, 4.2	added reference to notes on Web
		5.7	updated focus(temperature) formula
		5.15	updated info about DAT's
		A.2, A.3	more filter data; changed filter names
1.0.5	??	A.2, A.3	more filter data; comments S.v.Eck
1.0.6	16/03/02	2.9.1	Identified filters in standard calibration plan
1.0.6	16/03/02	2.9.1	Identified filters in standard calibration plan
1.0.7	23/03/02	2.8	Added comment about vignetting with Rc filter

Important Notice

This user manual not only describes the functionality and usage of the Wide Field Imager but also sketches how the instrument will be calibrated and the data be processed by ESO.
Please note that the latter is only gradually being ramped up. If the feasibility of the objectives or the observing strategy of your project(s) depends on the availability of these services, check the WWW page mentioned in Sect. 1.1 whether they are implemented already, or contact the 2.2-m Telescope Team (Internet: 2p2team@eso.org) for advice before submitting an observing proposal or executing an observing programme. Pipeline processing on an experimental basis is not expected to begin before the year 2000.
The scope and level of service observing are also currently under consideration. Please read the semi-annual Calls for Proposals for more up-to-date information.
Sections of this manual, which are not yet applicable, are marked with an asterisk (*) appended to the respective headings. We do welcome your feedback also on these sections (cf. Sect. 1.2)

Contents

1 Introduction **1**
1.1 Availability of this Document . . . 1
1.2 User Feedback and Inquiries . . . 1
1.3 Brief Characterization of the Instrument . . . 1
1.4 Some Project History . . . 2
1.5 How to use this Manual . . . 2
1.6 Bibliography . . . 3
1.7 Glossary . . . 3
1.8 Abbreviations and Acronyms . . . 4

2 Instrument Characteristics **5**
2.1 Optical Layout . . . 5
2.2 The Filter Storage and Exchange Mechanism . . . 6
2.2.1 The Shutter . . . 9
2.2.2 The Default Filter Set . . . 10
2.2.3 User-supplied Filters . . . 13
2.3 The Grisms . . . 13
2.4 The Instrument Rotator . . . 14
2.5 The Detector System . . . 14
2.5.1 The Science Mosaic . . . 15
2.5.1.1 Basic Characteristics . . . 15
2.5.1.2 Other properties . . . 20
2.5.2 The Tracker Chip . . . 23
2.6 The 2.2-m Telescope . . . 23
2.6.1 Optics and Image Quality . . . 23
2.6.2 Pointing and Tracking . . . 24
2.6.3 Autoguiding . . . 24
2.6.4 Finder Telescope . . . 25
2.7 Limiting Magnitudes . . . 25
2.8 Known Imperfections and Deficiencies . . . 25
2.9 Calibrations* . . . 26
2.9.1 Photometry* . . . 27
2.9.2 Spectroscopy* . . . 27
2.9.3 Polarimetry* . . . 27
2.9.4 Astrometry* . . . 27
2.10 Data Products* . . . 28

3 Operating Modes* **29**
3.1 Visitor Mode . . . 29
3.2 Service Mode* . . . 30
3.2.1 Scheduling* . . . 30
3.2.2 Execution of Observations* . . . 31

4 Preparing the Observations **32**
4.1 Defining Observations* . . . 33
4.1.1 Observing Templates* . . . 33
4.1.2 Observation Blocks* . . . 34
4.2 General Tools and Advice . . . 35
4.2.1 The Exposure Time Calculator . . . 35
4.2.2 Operational Overhead Times . . . 35

4.2.3 Guide Star Selection* . . . 37
4.2.4 Choosing the Detector Parameters . . . 38
4.3 Calibration Exposures* . . . 38
4.3.1 De-biassing . . . 38
4.3.2 Flat-Fielding . . . 38
4.3.3 Photometry . . . 40
4.3.4 Spectroscopy . . . 40
4.3.5 Polarimetry . . . 40
4.3.6 Astrometry . . . 40

5 Observing **41**
5.1 Safety . . . 41
5.2 Computers at the 2.2-m Telescope . . . 41
5.2.1 The TCS Workstation (w2p2tcs) . . . 41
5.2.2 The Instrument Control Workstation (w2p2ins) . . . 41
5.2.3 The Data Reduction Workstation (w2p2drs) . . . 42
5.2.4 Access to the Outside World . . . 42
5.3 Starting up DAISY+ . . . 42
5.4 Readying the Instrument . . . 43
5.5 Starting up the Telescope . . . 43
5.6 Daily Health Checks . . . 43
5.7 Focussing Telescope and Instrument . . . 43
5.8 On-line Creation of Observation Blocks* . . . 44
5.9 Broker for Observation Blocks (2p2BOB)* . . . 44
5.10 Executing an Observation Block* . . . 44
5.11 Defining and Executing Exposures within DAISY+ . . . 45
5.12 Keeping Track of the Observing Conditions . . . 46
5.12.1 Monitoring Telescope Tracking and Variations of Sky Transparency and PSF with the Autoguider . . . 46
5.12.2 The Meteorological Monitoring System . . . 46
5.13 Checking an Observation . . . 46
5.13.1 On the Real Time Display . . . 46
5.13.2 On the User Workstation . . . 47
5.14 Checking out the Detector . . . 48
5.15 Data Handling . . . 48
5.16 Operations Support Reports . . . 49
5.17 Utilities . . . 49
5.18 Shutdown Steps . . . 49
5.19 Cookbook . . . 50

6 Data Reduction and Calibration* **52**
6.1 Quality Control* . . . 52
6.1.1 Science Frames* . . . 52
6.1.2 Calibration Exposures* . . . 52
6.2 The Pipeline* . . . 53
6.2.1 Scope* . . . 53
6.2.2 Quality Control* . . . 54
6.2.3 Photometry* . . . 54
6.2.4 Spectroscopy* . . . 54
6.2.5 Polarimetry* . . . 54
6.2.6 Astrometry* . . . 54
6.3 The Calibration Database* . . . 54

6.3.1 Astronomical Data* . . . 54
6.3.2 Instrument Data* . . . 54
6.4 Off-line Data Reduction . . . 54
6.4.1 Bias Correction . . . 55
6.4.2 Flat Field Correction . . . 55
6.4.3 Photometry . . . 55
6.4.4 Spectroscopy . . . 55
6.4.5 Polarimetry . . . 55
6.4.6 Astrometry . . . 55

7 The Archive 56

A Appendices 57
A.1 Cosmetically Deficient CCD Columns . . . 57
A.2 Filter Transmission Curves . . . 59
A.2.1 Broad-band Filters . . . 59
A.2.2 Medium-band Filters . . . 60
A.2.3 Narrow-band Filters . . . 61
A.3 Filter Transmission Tables . . . 63
A.3.1 Broad-band Filters . . . 63
A.3.2 Medium-band Filters . . . 69
A.3.3 Narrow-band Filters . . . 73
A.4 Grism Transmission Curves . . . 75
A.5 Grism Transmission Tables . . . 75
A.6 Sample Observation Block . . . 75
A.7 Photometric Standards . . . 75
A.8 Polarimetric Standards . . . 75
A.9 Astrometric Standard Fields . . . 75
A.10 Sample FITS Headers . . . 75
A.10.1 Raw Frame . . . 75
A.10.2 Calibration Data* . . . 75
A.10.3 Pipeline-reduced Frame* . . . 75
A.11 Pointers to Sample Observations . . . 75

B Subject Index 76

List of Figures

1 Overview drawing . . . 5
2 Optical layout of camera . . . 6
3 The filter exchange and storage mechanism . . . 7
4 Filter geometry and CCD numbering . . . 8
5 Shutter timing errors . . . 9
6 Geometry of field covered by the grisms . . . 17
7 The detector array . . . 18
8 Quantum efficiency of mosaic CCD's . . . 19
9 Deviation of CCD response from linearity . . . 21
10 Exposure times as a function of magnitude . . . 36
11 Transmission curves for the broad-band filters . . . 59
12 Transmission curves for red medium-band filters . . . 60
13 Transmission curves for visual narrow-band filters . . . 61
14 Transmission curves for red narrow-band filters . . . 62

List of Tables

1 The Wide Field Imager in a nutshell . . . 2
2 Broad-band filters . . . 10
3 Polarizing filters . . . 10
4 Medium-band filters . . . 11
5 Narrow-band filters . . . 12
6 Summary of grism characteristics . . . 14
7 Hot CCD columns - top row of CCD's . . . 57
8 Hot CCD columns - bottom row of CCD's . . . 58
9 Dark CCD columns . . . 58
10 Transmission data for filter U/38 (ESO # 841) . . . 63
11 Transmission data for filter B/99 (ESO # 842) . . . 64
12 Transmission data for filter V/89 (ESO # 843) . . . 65
13 Transmission data for filter Rc/162 (ESO # 844) . . . 66
14 Transmission data for filter Ic/lwp (ESO # 845) . . . 67
15 Transmission data for filter Z+/60 (ESO # 846) . . . 68
16 Transmission data for filter 721/25 (ESO # 847) . . . 69
17 Transmission data for filter 753/18 (ESO # 848) . . . 70
18 Transmission data for filter 770/19 (ESO # 849) . . . 70
19 Transmission data for filter 790/25 (ESO # 850) . . . 71
20 Transmission data for filter 815/27 (ESO # 851) . . . 71
21 Transmission data for filter 838/25 (ESO # 852) . . . 71
22 Transmission data for filter 855/20 (ESO # 853) . . . 72
23 Transmission data for filter 915/28 (ESO # 854) . . . 72
24 Transmission data for filter OIII/8 (ESO # 859) . . . 73
25 Transmission data for filter Halpha/7 (ESO # 856) . . . 73
26 Transmission data for filter 665/12 (ESO # 858) . . . 74
27 Transmission data for filter SIIr/5 (ESO # 857) . . . 74

1 Introduction

1.1 Availability of this Document

The latest version of the WFI user manual is always accessible through the ESO - La Silla home page on the World Wide Web (URL: http://www.ls.eso.org), Telescope & Instrumentation section. Any recent changes in the areas covered by this document are also highlighted there. If you do not have convenient access to a WWW browser, you may retrieve the PostScript file by anonymous ftp access to ftp.ls.eso.org, file TBD. If all else fails, a printed copy can be requested from the Visiting Astronomers Section at ESO Headquarters in Garching (Internet: visas@eso.org). However, please note that new printed versions of the WFI user manual are prepared only after major revisions of the document.

1.2 User Feedback and Inquiries

ESO values and strongly encourages feedback from its users on the suitability of its equipment for their research. The WWW pages referred to above also describe (and include) means to contact relevant support staff. Electronic mail can also be sent directly to 2p2team@eso.org (Internet).

A printed copy of this manual will always be available in the control room of the 2.2-m telescope. Any observations about this document can be written into that copy which, therefore, should not be removed.

1.3 Brief Characterization of the Instrument

The WFI is a focal reducer-type camera which is permanently mounted at the Cassegrain focus of the 2.2-m MPG/ESO telescope at La Silla. It has a field of view with a diameter of almost 0.8 degree (detector coverage: $(34 \times 33)\,\mathrm{arcmin}^2$) and therefore in this regard exceeds any other current La Silla or VLT instrument by at least a factor of 2. A mosaic of 2×4 CCD detectors with narrow inter-chip gaps yielding a filling factor of 95.9% offers excellent sensitivity from the atmospheric UV cut-off to the near IR. The pixel size of 0.24 arcsec will only under the most superb seeing conditions undersample the point spread function. The filter storage and change mechanism can accommodate up to 50 filters simultaneously. The default filter set includes a large number of medium- and narrow-band filters that are specifically selected to support the determination of photometric redshifts of distant objects. Linear polarisation measurements are possible in a broad blue band. Two grisms for slitless field spectroscopy at low dispersion will be made available later.

Since, apart from the camera shutter, the filters are the only moveable parts, the WFI is very easy to use. One FITS image has a size of about 142 Mbyte. In spite of this, such an image can be read in less than half a minute with a readout noise as low as $\sim 4.5\,\mathrm{e}^-$/pixel which, for most applications, is still negligible in comparison with the sky shot noise.

A more comprehensive overview in tabular form is provided in Table 1.

The Wide Field Imager in a Nutshell

Field of view:	**(34×33) arcmin^2**
Pixel scale:	**0.238 arcsec/pixel**
Detector:	**mosaic of eight 2k $\times$ 4k CCD's**
Filling factor:	**95.9%**
Read-out time:	**27 seconds**
Read-out noise:	**4.5$\pm$0.1 e$^-$/pixel**
(Inverse) gain:	**2.0$\pm$0.1 e$-$/ADU**
Dynamical range:	**16 bit**
Saturation limit:	**$>$ 200.000 e$^-$/pixel**
Telescope aperture:	**2.2 m**
Telescope focus:	**Cassegrain (f/8)**
Instrument F ratio	**5.9**
Peak overall througput:	**TBD % at TBD nm**
Useful wavelength range:	**atmospheric cutoff through 1 μm**
Limiting magnitude:	**V - TBD mag (5-σ detection in TBD min. at 1" seeing)**
Overall intrinsic image quality:	**0.4 arcsec**
Overall geometrical distortions:	**$\leq$0.08%**
No. of simult. mountable filters:	**50**
Slitless spectroscopy:	**4.5 (5.7) nm resolution at 400-640 (650-850) nm**
Imaging linear polarimetry:	**@470 nm (TBC)**
Raw data format:	**FITS (with extensions), 142 Mbyte/file**

Table 1: The Wide Field Imager - an overview

1.4 Some Project History

In 1995 November the Working Group *La Silla 2000* and ESO's Scientifc Technical Committee identified a strong need of the ESO community for a modern wide-angle camera and encouraged ESO to make such an instrument available. In response to this initiative the present WFI was proposed as a possible realisation of such wishes by the Max-Planck Institut für Astronomie in Heidelberg (MPI-A). The resulting project was, then, jointly executed by the MPI-A (optics, mechanics), the Osservatorio Astronomico di Capodimonte (cost of the CCD mosaic), the Optical Detector Group (detector system) and the Project Support Group (optical design) of the Instrumentation Division at ESO Headquarters in Garching, and the 2.2-m Telescope Team at La Silla (interfacing to and development of instrument and telescope control software).

1.5 How to use this Manual

This manual is intended to assist the user throughout the life cycle of an observing programme with the WFI. In fact, its ambition is that it is unlikely that any of the following can be done more conveniently or effectively without reading this manual than with reading it:

Preparation of proposals: Sects. 2 (description of the instrument and its capabilities) and 3 (for the decision between visitor or service mode)

Preparation of observations: Sects. 4 (for the preparation of the exposures to be made) and 5 (for a preview of the practical execution of the observations)

Execution of observations: Sect. 5

Data reduction and calibration: Sect. 6

1.6 Bibliography

[1] WFI Calibration Plan, Doc. No. LSO-PLA-ESO-22401-00001

[2] WFI Operations Plan, Doc. No. LSO-PLA-ESO-22401-00002

[3] FIERA user guide (TBD)

[4] RTD user guide (TBD)

[5] Thommes E., Meisenheimer K., Fockenbrock R., Hippelein H., Röser H.-J. 1997, in R.E. Schielicke (ed.): Reviews in Modern Astronomy, Vol. 10, p. 297

1.7 Glossary

Note that the operations scheme for the WFI emulates the VLT operations model. Therefore, this document partly uses VLT-like jargon. However, in many instances this similarity exists only at the conceptual level whereas the actual implementation may be quite different.

Autoguider: An imaging device which permits the relative position of the image of an isolated star to be monitored at a frequency of some Hertz. Any deviations from the nominal position are fed back to the TCS in order to be compensated for by corresponding telescope offsets (Sect. 2.6.3). The corrections are relative to the tracking of the telescope.

DAISY+: The software system via which the user controls the instrument (Sect. 5.3) and, for focussing only, the telescope.

FIERA: The electronics system that prepares the CCD for an exposure, starts and supervises the exposure, reads the data, writes them to the memory of the Real Time Display and sends them to the instrument work station where the files are written to disk in FITS format (Sect. 2.5).

FITS: A standard for the format of image files and their associated ancillary parameters (Sects. A.10.1 and A.10.2).

Observation Block: The smallest unit of action that DAISY+ can execute (Sect. 4.1.2). It consists of one or several Observing Template signature files.

Observing Template: The 'subatomic' units that constitute an Observation Block. Often they imply only a single exposure, though some also support more complex coordinated operations of both WFI and the telescope (Sect. 4.1.1).

Real Time Display: An image display where the images are displayed as they are read out of the detector (Sect. 5.13.1).

Observing Template Signature File: An ASCII file that contains the parameters with which the associated Observing Template shall be executed.

Seeing Monitor: A small telescope which on the basis of differential image motions measures the seeing (Sect. 5.12.2).
(URL: http://epu.ls.eso.org/lasilla/dimm/meteo/).

Service Observing: The successful applicants supply the Observatory with Observation Blocks which are executed by ESO staff without presence of the applicants.

TCS: The software system used to control the telescope. For autoguiding, it uses the separate tracker of the WFI and together with DAISY+ shares the controller over the single instrument shutter.

Visitor Mode: In this alternative mode to service observing, the applicants themselves carry out their observing program.

1.8 Abbreviations and Acronyms

ADU	Analog Digital Unit
ASCII	American Standard Code for Information Interchange
A/D	Analog-to-Digital
CCD	Charge Coupled Device
DAISY+	Data Acquisition Integrated SYstem "plus"
DAT	Digital Audio Tape
DLT	Digital Linear Tape
ESO	European Southern Observatory
FIERA	Fast Imager Electronic Readout Assembly
FWHM	Full Width at Half Maximum
FF	Flat Field
FOV	Field Of View
ftp	file transfer protocol
GUI	Graphical User Interface
IDL	Interactive Data Language
IRAF	Image Reduction and Analysis Facility
LAN	Local Area Network
MIDAS	Munich Image Data Analysis System
MPG	Max-Planck-Gesellschaft
M1, M2	primary and secondary, respectively, mirror of the telescope
NS	Night Sky
NTT	New Technology Telescope
OB	Observation Block
PRNU	Pixel Response Non-Uniformity
PSF	Point Spread Function
QE	Quantum Efficiency
rms	root mean square
RAID	Redundant Array of Inexpensive/Independent Disks
RAM	Random Access Memory
RTD	Real Time Display
TBC	To Be Completed, To Be Confirmed
TBD	To Be Decided, To Be Done
TCS	Telescope Control System
URL	Uniform Resource Locator (a WWW address)
VLT	Very Large Telescope
WFI	Wide Field Imager at the 2.2-m telescope
WWW	World Wide Web

2 Instrument Characteristics

The Wide Field Imager at the 2.2-m MPG/ESO telescope on La Silla (WFI) was designed to map full-moon-sized fields at a sampling adequate even under very good seeing conditions and with the characteristics of front-line optical detectors. This manual attempts to describe how the scientific potential of the instrument can be exploited. A schematic overview of its main components is provided in Fig. 1.

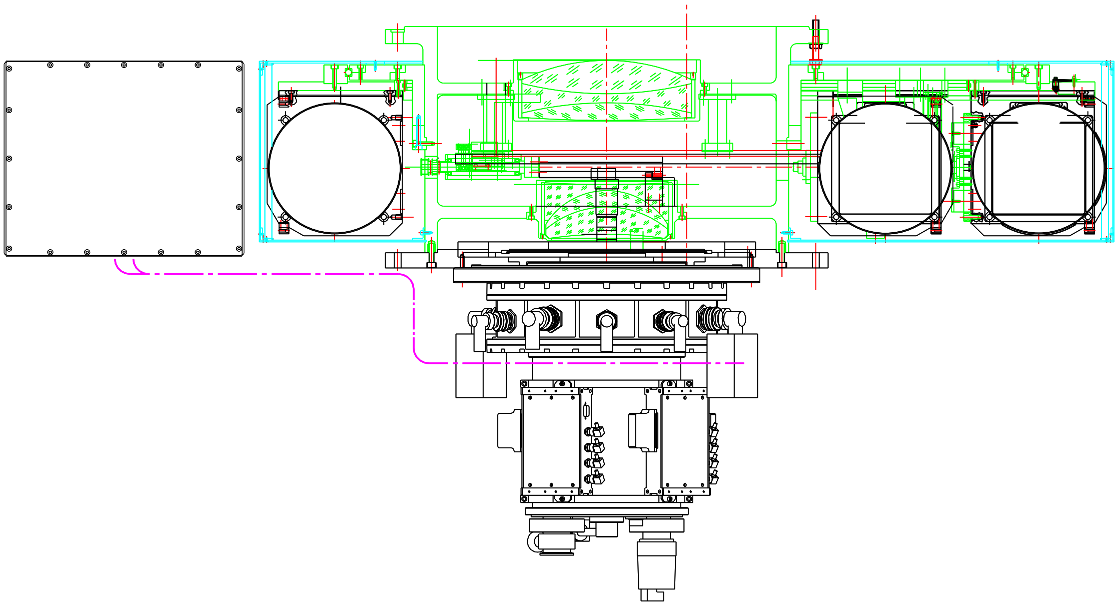

Figure 1: The main components of the WFI: The outer circles are cross sections of the filter storage ring (cf. Fig. 3). The lenses of the focal reducer are hatched (cf. Fig. 2). The ring below is the flange which attaches the dewar to the instrument. The short cylinder with the vacuum connectors, through which the CCD's communicate with the outside world, is the cryostat head and contains the detectors. The liquid nitrogen needed for cooling the detectors is contained in the tank below to which the pre-amplifier boxes are attached. The large rectangle on the left is the box with the FIERA detector control electronics (Sect. 2.5). It also serves to counterbalance the torque exerted on the telescope by the off-centre position (with respect to the optical and mechanical axis of the telescope) of the filter storage ring (see also Fig. 3). Most cables, the hoses for the water cooling of FIERA, an emergency vacuum pump for the dewar, and several minor components are not shown. Also omitted are the protective shutter above the top lens and the support system for grisms which can be mounted in front of the first lens

2.1 Optical Layout

The instrument is installed at the Cassegrain focus of the 2.2-m telescope. Six lenses in two blocks, i.e. two triplets (Fig. 2), provide a field of view (FOV) with a diameter of nearly 0.8°. Over this FOV and the wavelength range from 350 to 1000 nm, 80% of the energy is encircled within less than 15 μm (i.e., the CCD pixel size, Sect. 2.5.1); the only exception is the combination of wavelengths above ∼900 nm and off-axis distances in excess of ∼0.35°. The throughput is near 80% from 400 to 1000 nm but drops steeply to 45% at 350 nm. (Similar performance is also possible from 1050 to 1350 nm and from 1400 to 1800 nm [not simultaneoulsy because of different focal planes] so that the WFI can, in principle, also be equipped with an array of near- to mid-IR detectors.) The focal reducer characteristics of this F/5.90 camera change the intrinsic telescope plate scale of 2.34 arcsec/mm to

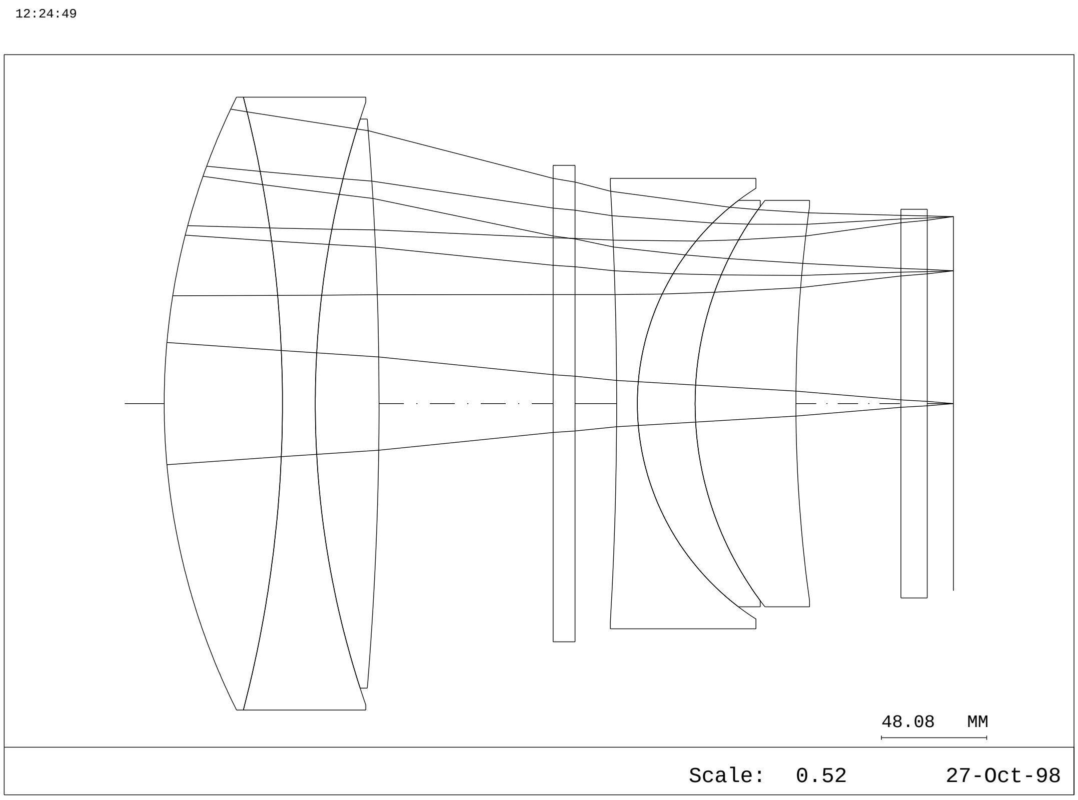

Figure 2: The optical layout of the focal reducer. From left to right are shown the first triplet, a filter, the second triplet, the dewar entrance window, and the focal (detector) plane

15.9 arcsec/mm or 0.238 arcsec per 15-μm pixel. The scale is constant to better than 0.08% across the focal plane. This means that even without correction for this variation in scale, surface photometry is accurate to about 2 mmag. Sky concentration, which is the typical shortcoming of focal reducers, amounts to no more than about 2% (peak to peak).

2.2 The Filter Storage and Exchange Mechanism

The WFI can accommodate up to 50 filters at any one time. Those not in the beam (only one filter can be in the beam at a time) are stored in a turnable ring around the beam. There, they are kept rotated through 90 degrees about a radial axis and with respect to the in-beam position (Fig. 3). This maximizes the number of filters that the ring can hold in a single layer, and it minimizes the settling of dust on them. A filter grabber inserts the filters in the beam and moves them back into the storage ring (Fig. 3).

The filter ring can rotate at a rate of one full turn per 2 minutes. However, it is not possible to move directly from position 1 to 50 or vice versa. Since the shortest path cannot be used, if it would require this transition, the ring turning time is always about 2.4 seconds times the difference in filter position numbers. To this, 45 seconds need to be added for taking one filter out of the beam and inserting the other one.

Note that requests for the mounting of other filters in the instrument are considered during daytime *only* and need to be made before 8 a.m. using the WWW-based report system (Sect. 5.16). Given that the WFI can hold up to 50 filters simultaneously, a bit of planning would usually make such a request unnecesaary after the initial instrument setup has been made for the observing run.

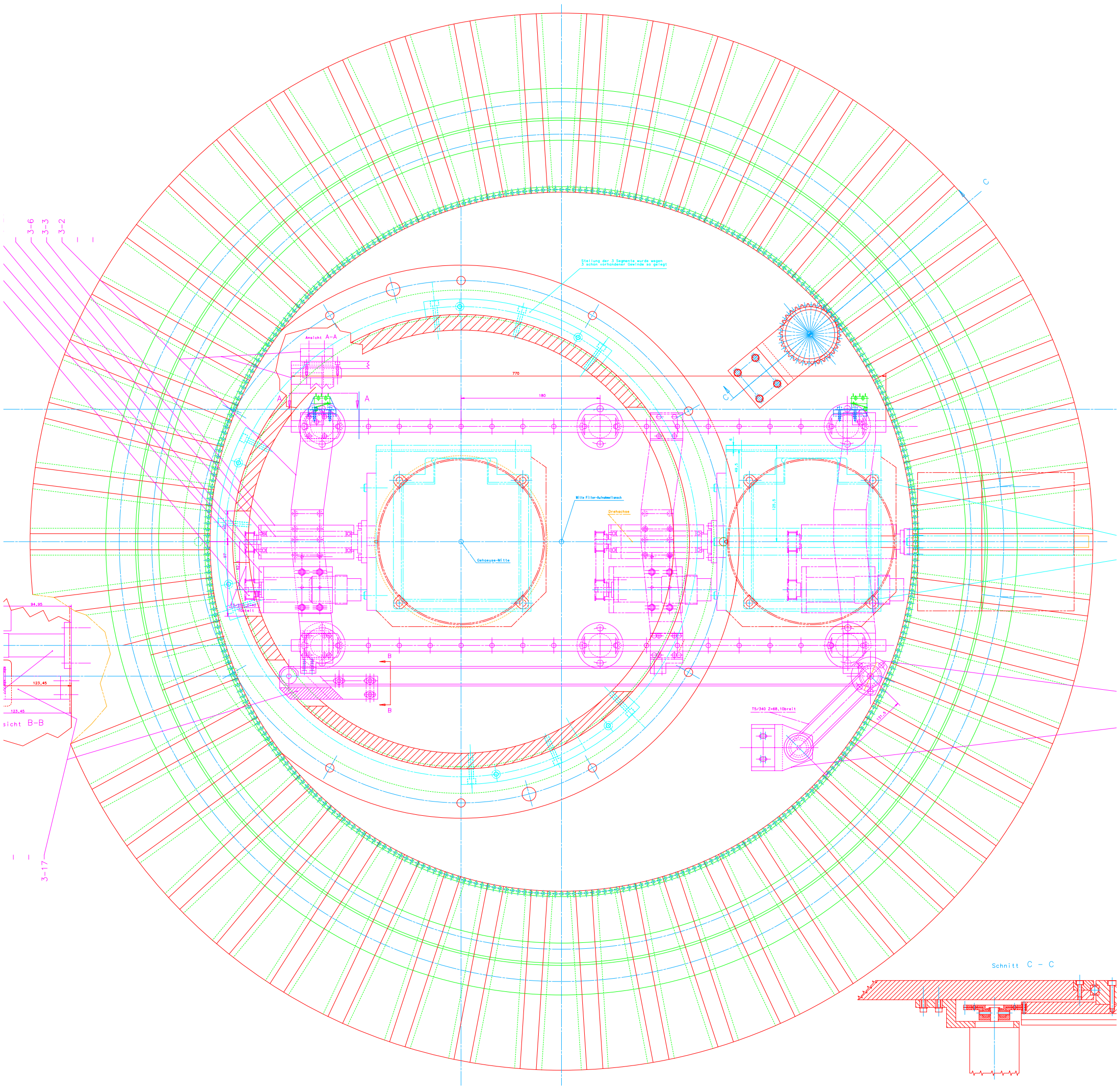

Figure 3: The filter exchange and storage mechanism as seen from the top of the instrument. The large (rotatable) outer ring contains slots for 50 filters which are stored vertically. On the right-hand side a filter, when requested, is pulled out of the ring, rotated through 90 degrees into the plane of the drawing (this position is shown), and finally shifted to the left into the optical beam and operating position (this position is also shown). Note that the filter storage ring is not centered on the optical axis of telescope and instrument. The resulting net torque requires that the telescope balancing is checked when the instrument is rotated out of the default position angle

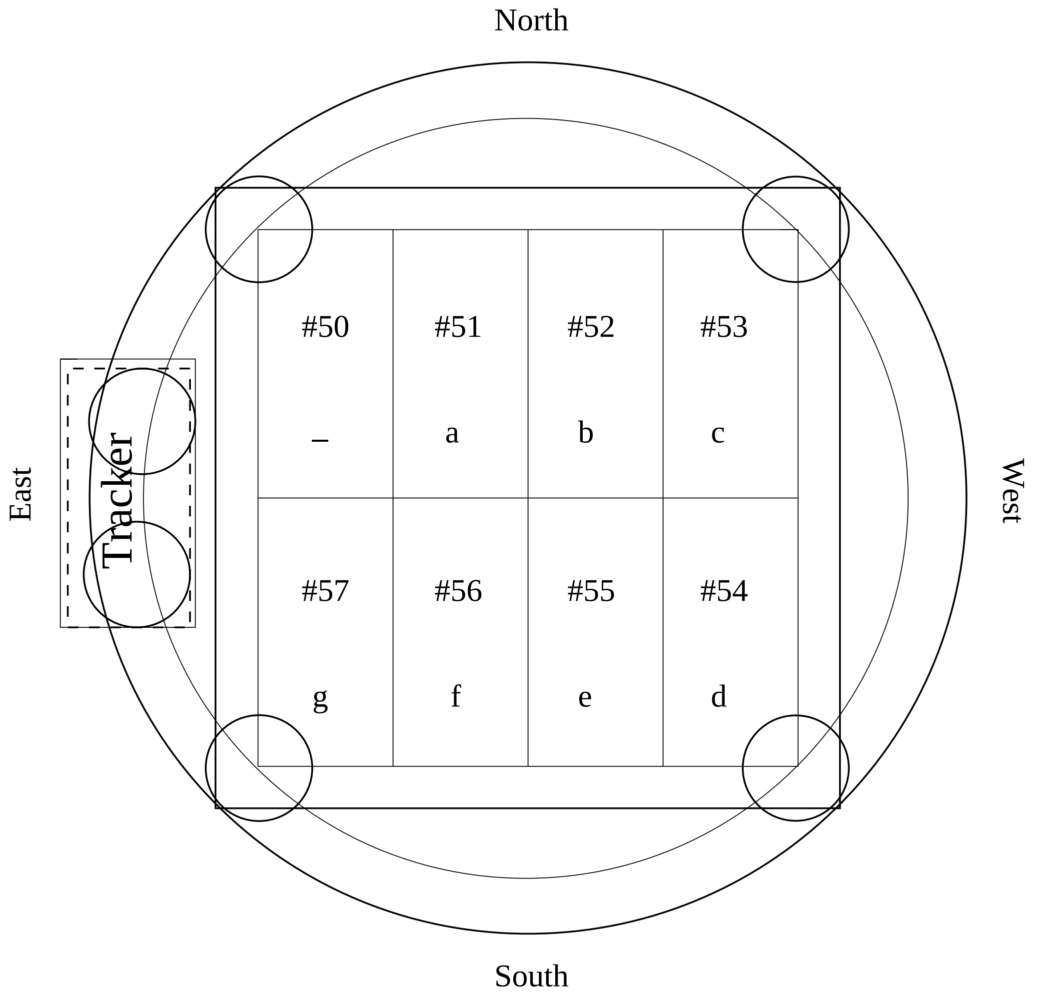

Figure 4: Schematic projection of the detector plane onto the filter plane. The thin rectangles show the CCD's in the mosaic (Sect. 2.5.1) and the tracker CCD (Sect. 2.5.2), respectively, *in the detector plane*. Because the filters are in the converging beam, the mosaic projects *in the filter plane* onto the thick (outer) square. In the case of medium- and narrow-band filters, their dimensions closely match the thick square. The dashed rectangle corresponds to the auxiliary glass filter used for autoguiding (Sect. 2.2). The large (inner) thin and (outer) thick circles delineate the limits of the optical field of view in the detector and filter plane, respectively.
In the filter plane, point sources reach the dimension of the small thick circles. As can be seen, stars falling right onto a corner of the mosaic are just not vignetted. By contrast, the two small circles at the position of the tracker CCD indicate the two most extreme positions between which there is essentially no vignetting. All other parts of the tracker CCD are more or less vignetted but, depending on the brightness of the star, still useful for autoguiding.
Broad-band filters are circular in shape and have the diameter of the outer (thick) circle and therefore cover both the mosaic and the tracker CCD.
The cardinal directions are indicated as projected onto the sky.
Note also the two identification schemes for the CCD's. Numbers denote a physical chip, letters the physical location within the mosaic. Except for the "_", which in MIDAS is replaced with a blank, the letters are the same as appended to the root file name when they are read into MIDAS by commands INTAPE/FITS or INDISK/FITS

The broad-band filters are circular in shape and cover both the CCD mosaic used for scientific imaging (Sect. 2.5.1) and the tracker CCD serving as an autoguider (Sect. 2.5.2). The interference filters are square, measuring 152 mm on a side which is just sufficient to avoid major vignetting of the science mosaic (Fig. 4). Their mount also holds a smaller filter (Fig. 4) which intersects the beam only towards the tracker CCD (Sect. 2.5.2). The central wavelength of this auxiliary filter approximates the one of the main filter. This reduces the cost of the science filters, which already are the largest ones currently available, but also differential atmospheric effects between guide star and target. These auxiliary filters are broad-band glass filters and, therefore, have a larger throughput than the interference filters so that narrow-band observations can use guide stars of the same magnitude as broad-band observations. Since main and auxiliary filter are mounted in one and the same frame, their combination is fixed.

2.2.1 The Shutter

Both the science mosaic (Sect. 2.5.1) and the tracker CCD (Sect. 2.5.2) share the same shutter. It consists of a rotating, roughly semi-circular disk. It can operate at two different speeds. In view of the large size of the shutter the faster speed is only used for exposures shorter than 2 seconds in order to reduce fatigue and wear of the mechanics. The selection of the shutter speed is done automatically by the control software and, therefore, completely transparent to the user.

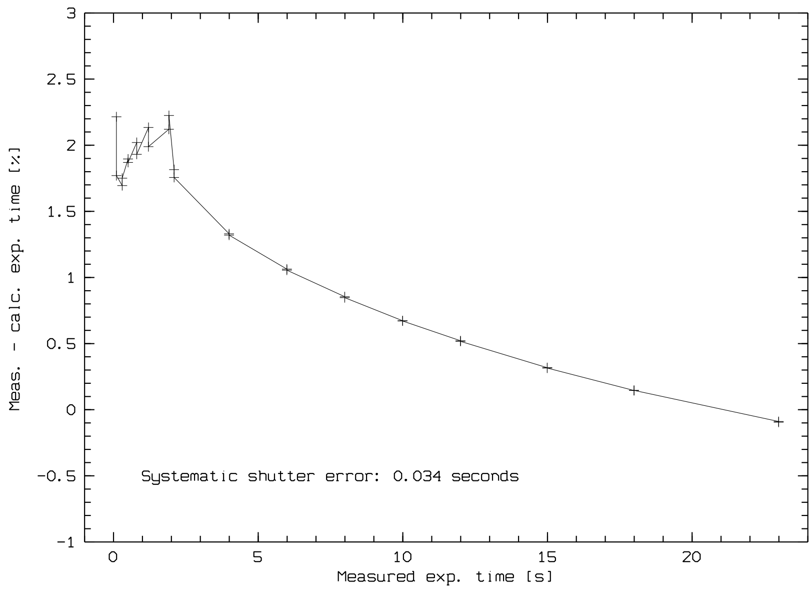

Figure 5: The fractional difference (in percent) between (i) the computed (by means of a linear regression analysis) shutter open time and (ii) the one measured by the instrument electronics plotted versus exposure time. From the difference the systematic error of 0.034 sec is already subtracted. The exposure time in the FITS headers is the measured one and, therefore, has to be corrected for both the systematic error, which is independent of the exposure time, and the fractional error shown in the graph. The small dicontinuity around exposure times of 2 seconds is due to the change-over between the two shutter speeds (cf. Sect. 2.2.1

From the ratio of short and long exposures taken both with a β-light and on the twilight sky, only an upper limit of 0.2% for the nonuniformity of the shutter motion could be determined. The shutter error is of the order of 0.03 sec, i.e. the actual shutter open time is on average 0.03 sec shorter than

Table 2: The default broad-band filters; the focus offsets refer to the B-band filter and are defined as: offset = $f_{\rm other} - f_{\rm B}$

Filter No.	Filter name	λ_c [nm]	FWHM [nm]	Comment	Focus offset [M2 encod. units]
841	U	355	55	interf.; simil. to Strømgren u	
842	B/99	456	99	interfer.; high effic., avoids 400 nm	±0
843	V/89	540	89	BG39/2 + GG495/2; approx. V_J	–140
844	Rc/162	652	162	OG 570/3 + Calflex; approx. R_C	
845	Ic/lwp*	784	lwp	RG 780 + CCD; approx. I_C	–55
846	Z+/70	960	70	LPF 925 + CCD	

* This is a long-wavelength passband (lwp) filter. Therefore, a FWHM cannot be provided and the stated λ_c actually is the short-wavelength edge.

Table 3: Same as Table 2 except for default polarizing filters

Filter No.	Filter name	λ_c [nm]	FWHM [nm]	Comment	Focus offset [M2 encod. units]
	BV	470.	200.	BG 39/3 no polarizer	
	BV-0	470.	200.	BG 39/3 + polarizer 0°	
	BV-30	470.	200.	BG 39/3 + polarizer 30°	
	BV-60	470.	200.	BG 39/3 + polarizer 60°	

measured by the instrument itself and stated in the FITS header. After correction for this shutter error, there are still some systematic residual errors as shown in Fig. 5. Note that an error of 1% for an exposure time of 0.2 sec translates into an absolute error of only 2 msec which for a shutter of this size is excellent.

2.2.2 The Default Filter Set

The full complement of filters foreseen to be mounted by default is fully characterized in Sects. A.2 and A.3. An overview is given in Tables 2 to 5. However, please **note** that so far only a subset has been delivered by the manufacturer. Filters listed without filter number may not yet exist; their parameters are for information only and do not establish a committment by ESO to eventually offer them. For the actually available filters and most up-to-date status information **always** refer to the WWW page mentioned in Sect. 1.1.

The numerous narrow-band filters contained in it have been chosen such as to permit photometric redshifts to be determined of distant emission line galaxies and quasars. It is based on three atmospheric windows that are relatively free of night-sky emission lines: 694-706 nm (`A`), 814-826 nm (`B`), and 910-926 nm (`C`). If a strong emission line falls into one of them and another emission line is detected in a second narrow-band filter, the spacing between the filter passbands fixes the redshift if the spacing is chosen such that only one combination of redshift and wavelength difference between major emission lines can lead to such a double coincidence (cf. [5]). The following table shows the redshifts at which the given lines would fall into one of the windows `A, B,` or `C`:

Table 4: Same as Table 2 except for the default medium-band filters

Filter No.	Filter name	λ_c [nm]	FWHM [nm]	$\Delta\lambda/\lambda_c$ [%]	Comment	Focus offset [M2 encod. units]
	395m	395	14	3.5	[OII]; $z = 0.04...0.10$ (A)	
	410m	410	20	4.9		
	428m	428	20	4.7		
	446m	446	20	4.5		
	464m	464	15	3.2	[OII]; $z = 0.23...0.27$ (B)	
	486m	486	32	6.5		
	506m	506	12	2.2	[OIII]; $z = 0....0.02$	
	520m	520	20	3.9	[OII]; $z = 0.37...0.42$ (C)	
	540m	540	24	4.4	[OIII]; $z = 0.06...0.10$ (A)	
	573m	573	24	4.4		
	605m	605	21	3.5	[OII]; $z = 0.59...0.65$ (B)	
	622m	622	19	3.1	[OIII]; $z = 0.23...0.26$ (B)	
	643m	643	26	4.0		
	664m	664	12	1.8	$H_\alpha; z = 0.004...0.02$	
	675m	675	20	3.0		
	690m	690	20	2.9	[OII]; $z = 0.82...0.88$ (C)	
	709m	709	22	3.1	NS window: H_α; $z = 0.06...0.10$ and [OIII]; $z = 0.39...0.44$	
847	721/25	721.8	25.6	3.9		–40
	731m	731	25	3.4		
848	753/18	753.2	18.3	2.7	M-star peak	–25
849	770/19	770.5	19.4	2.6	M-star trough, NS window	–25
	787m	787	40	5.1		
850	790/25	790.6	25.9	3.7		–20
851	815/27	815.4	27.6	2.9	NS window: $H_\alpha; z = 0.23...0.26$ and [OIII]; $z = 0.60...0.65$	–20
852	838/25	838.1	25.9	3.6		–10
853	855/20	855.6	20.9	1.8	M-star trough, NS window	–20
	885m	885	30	3.4		
854	915/28	915.2	28.6	3.5	NS window: $H_\alpha; z = 0.37...0.42$ and [OIII]; $z = 0.79...0.85$	–25:

Table 5: Same as Table 2 except for the default narrow-band filters. The homogeneity of the passbands over the full size of the filters appears to be much better than 1% in central wavelength. Because the filters are in a mildly converging beam, the effective central wavelengths are about 0.1% less than the manufacturers' measurements shown below. The comment columns have the following meaning: (1) The redshifted line: If the object has the redshift given in the last column, i.e. 4, this line will appear in the filter. (2) The referred-to reference spectral window as defined in Sect. 2.2.2 and by the last three filters in this table. (3) The line falling at the given redshift into the reference window given in the previous column, i.e. 2. (4) The redshift range over which this double coincidence can occur

Filter No.	Filter name	λ_c [nm]	FWHM [nm]	Comments (1)	(2)	(3)	(4)	Focus offset [M2 encod. units]
	374n	374	5	[OII]	–	–	$\simeq 0$	
	399n	398	4	[OII]	A	Hα	0.070±0.005	
	466n	398	5	[OII]	B	Hα	0.249±0.006	
859	OIII/8	502.4	8.0	[OIII]	–	–	$\simeq 0$	–15
	522n	521	8	[OII]	A	[OIII]	0.402±0.007	
	536n	535	6	[OIII]	A	Hα	0.070±0.005	
	609n	609	9	[OII]	B	[OIII]	0.638±0.008	
	625n	625	6	[OIII]	B	Hα	0.249±0.006	
856	Halpha/7	658.8	7.4	Hα	–	–	$\simeq 0$	–10
858	665n/12	665.6	12.1					–25
855	SII	676	5	[SII]	–	–	≥ 0	
857	SIIr/5	675.8	5.2	[SII]	–	–	≥ 0	0
	683n	683	11	[OII]	C	[OIII]	0.837±0.009	
	702n	702	7	–	$\equiv$ A	–	–	
	820n	820	8	–	$\equiv$ B	–	–	
	920n	920	9	–	$\equiv$ C	–	–	

Line	Window A 694-706 nm	Window B 814-826 nm	Window C 910-926 nm
Hα	0.070±.0005	0.249±0.006	0.402±0.007
[O III] λ5007	0.402±0.007	0.638±0.008	0.837±0.009
[O II] λ3727	0.884±0.009	1.200±0.011	1.468±0.012
Ly-α	4.77±0.03	5.75±0.03	6.57±0.04

Note that the effective filter passband changes with position of the objects in the field of view because the filters are mounted in the converging beam. The narrower the passband, the more important this effect is.

Typical sky background count rates at different lunar phases of a number of representative filters are compiled in the following table:

Filter	λ_c [nm]	$\Delta\lambda$ [nm]	Sky background count rates ADU's/pix/s		
			New moon	Half moon	Full moon
U	355	55	0.1		1.5
B	455	110	0.3	2.3	16
816m	816	24	0.2	0.4	
913m	913	30	0.3		

2.2.3 User-supplied Filters

Users are welcome to bring their own filters but they are urged to contact the 2.2-m Telescope Team (2p2team@eso.org) before submitting an observing proposal or purchasing the filters. The following constraints need to be met but are not guaranteed to be sufficient:

- The *optical* thickness must not deviate by more than 1 mm from the one of the nominal filter used for the optical design (11 mm BK7).
- In case of very-broad band filters, the Abbe number of the substrate must be larger than 55.
- Size: (a) 6" × 6" plus broad-band auxiliary filter or (b) 210 mm diameter
- Holder: Only holders made by the Max-Planck-Institut für Astronomie in Heidelberg are admissable. For details contact the 2.2-m Telescope Team.

2.3 The Grisms

Please **note** that the grism mode will be commissioned only in Period 63. For up-to-date information, kindly check the WWW page given in Sect. 1.1.

Two grisms are available for slitless field spectroscopy which can be a powerful technique especially for the recognition of emission line objects or for the separation of objects that do or do not fall into a certain redshift range. Their basic properties are summarized in Table 6. Throughput curves and tables are provided in Sect. A.4 and A.5, respectively. Owing to the limited size of the grisms, the unvignetted spectroscopic field of view is limited by a circle of 0.31 degree radius, i.e. the corners of the CCD mosaic (Sect. 2.5.1) are not covered. Moreover, since the grooves only extend over 80% of the diameter of the grism, a strip of width 0.12 degree on the Eastern side (on the sky) is also not useful. At position angle zero of the instrument (North at top of image), which is the default (Sect. 2.4), the dispersion direction runs East-West. A graphical representation of the geometry is provided in Fig. 6.

Table 6: Calculated (i.e. not yet measured) primary characteristics of the grisms. All figures refer to the average over (i) the full wavelength range, (ii) 70% of the field, and (iii) a seeing of 1 arcsec. A shorter wavelength, a smaller distance from the optical axis, and better seeing can each lead to improvements of 5-20%. Image quality is the width of the spectrum of a point source perpendicular to the dispersion direction (one pixel corresponds to 0.24 arcsec)

Grism name	Wavelength range [nm]	Blaze [nm]	Dispersion [nm/pixel]	Spectr. Resol. [nm]	Image Quality [pixel]
B50	400-650	370	0.81	4.5	5.5
R50	650-850	590	0.81	5.7	7.1

Not only the first order, but also orders Nos. 2, 0, –1, and –2 appear. The zeroth order is fairly strong but, owing to its very small extent, very useful for setting the zeropoint of the wavelength scale. Because of the grism blaze, all orders other than the first one receive only about 2% of the light.

Grisms can only be exchanged, mounted, or dismounted with the instrument taken off the telescope. Therefore, in a given night either no grism or only one grism can be used.

Grisms can be combined with any filter. The narrower the filter passband is, the shorter the spectra will be, thereby reducing the degree of crowding. Filters also provide the only means of suppressing contaminating neighbouring spectral orders. The drawback of narrow filters is obviously the reduced spectral coverage (or, for a given spectral feature, the reduced redshift coverage). It may be overcome by multiple observations through filters adjacent in wavelength. The negative effects of overlapping spectra can also be alleviated by taking spectra at two position angles differing by 90 degrees (Sect. 2.4).

2.4 The Instrument Rotator

The Cassegrain adapter of the 2.2-m telescope includes a rotator that permits the instrument mounted to be rotated through 90 degrees. Currently, it can only be operated manually (with the telescope pointing to the zenith); a motor is expected to become available in 1999. Position angles can be set to better than 0.5 degree (TBC). Observers wishing to use a wide range of position angles are, however, advised to keep in mind that the non-axisymmetric mass distribution of the instrument (Figs. 1 and 2) implies that the telescope balancing ought to be checked because otherwise pointing and tracking performance would be seriously degraded. This can only be done at daytime.

Given the square dimensions of the science detector mosaic (Sect. 2.5.1), most observing programs would not normally require a particular position angle of the WFI. The need to overcome crowding in the case of grism field spectroscopy or to use a particular guide star may be two of the very rare exceptions. However, ESO does not supply astrometric calibrations (Sect. 4.3.6) for any position angle other than the default one. If it turns out that a full astrometric re-calibration is needed after a temporary change of position angle, modifications of the position angle may be prohibited by the 2.2-m Telescope Team Coordinator.

The default position angle is zero, i.e., on the mosaic North is at the top and East to the left.

2.5 The Detector System

The most important components of the detector system are the science mosaic (Sect. 2.5.1), the tracker CCD (Sect. 2.5.2), and the controller, FIERA. The latter is ESO's own design and product and belongs to the most powerful devices of its kind. It is largely the performance of FIERA which has permitted the WFI to come into existence because without FIERA such a large array could not easily be used effectively or without degradation of the data quality. However, when using the WFI, the observer does not directly notice FIERA. Therefore, instead of a desription of FIERA only reference to a separate publication [3] is made here.

Cooling of the detector system is provided by a liquid nitrogen-filled bath cryostat. Because of the large dimension of the mosaic and, therefore, the entrance window to the dewar, the hold time of the cryostat is less than 24 hours so that the cryostat has to be re-filled twice a day. The mosaic is kept at a temperature of 169±0.1 K. If the temperature rises above a value of about 175-180 K, a dramatic increase of the number of hot pixels by up to 2 orders of magnitude or more is to be expected.

Since at times of high humidity ice can form on the dewar entrance window, it is continually flushed with a flow of dry nitrogen gas when the meteorological conditions are critical.

2.5.1 The Science Mosaic

2.5.1.1 Basic Characteristics

The detector system for scientific exposures is an array of 2×4 *CCD44* chips by EEV which have 2k × 4k 15-μm pixels each. They are three-side buttable; but there are gaps of $\sim$ 98±2 pixels along the long and of ~30±2 pixels along the short side of the chips (Fig. 7).

In order that on-chip binning (cf. below) yields consistent results for all binning factors supported, the actual number of light-sensitive pixels per chip is 2046 in the horizontal (East-West) and 4098 in the serial (Nort-South) direction. In addition, there are 48 pre- and also 48 overscan pixels in the horizontal direction and 30 vertical overscan pixels which can be used for monitoring the bias level. The mosaic, therefore, comprises $8184 \times 8196 = 67{,}076{,}064$ light-sensitive pixels and subtends an angle of roughly $0.57 \times 0.54 = 0.31$ square degrees, i.e. matches the largest possible square contained in the optical FOV (Sect. 2.1).

In a hyper-pixel grid covering the full field of view, the southeastern most light-sensitive pixels of each CCD fall on pixels with the following X/Y coordinates:

CCD No.	X	Y
50	2	4130
51	2149	4127
52	4293	4125
53	6437	4128
54	6437	3
55	4292	1
56	2149	1
57	5	6

Both the alignment of the CCD's and the optical quality of the camera are sufficiently good that images, that at similar hour angles were taken with relative offsets of up to a few tens of arcseconds and re-assembled in this way, can by a simple translation (i.e., without rotation or other rebinning) be aligned to about 0.5 arcsec rms over the entire field of view. The chip that is rotated by far the most w.r.t. to the mean position angle is No. 50 with a misalignment of order 0.1 degree.

The surfaces of all 8 chips are confined between two planes ~80 μm apart. The mean plane of the mosaic has been carefully aligned with the focal plane so that, if the focus is properly set (Sect. 5.7), the peak-to-peak difference in optimal focus does not exceed 15 M2 encoder steps (Sect. 5.7) near the zenith. This is well within the focal depth of about 50 encoder units. At hour angles of ± 2.5 hours flexure adds up to another 25 encoder units to the above figure for the focal tilt of 15 encoder units.

The CCD's are notable for their high quantum efficiency from the atmospheric cut-off and through the visual part of the spectrum (Fig. 8). There are slight chip-to-chip variations which are probably due to differences in the effectiveness of the anti-reflection coating.

The pixel response non-uniformity (PRNU) depends on the wavelength because redder photons create electrons deeper within the CCD. Towards longer wavelengths, there is also some fringing. Some indicative figures are given in the following table:

Wavelength nm	PRNU % rms
320	2.3
400	0.9
550	0.8
700	0.9
800	1.6
900	2.7
1000	7.0

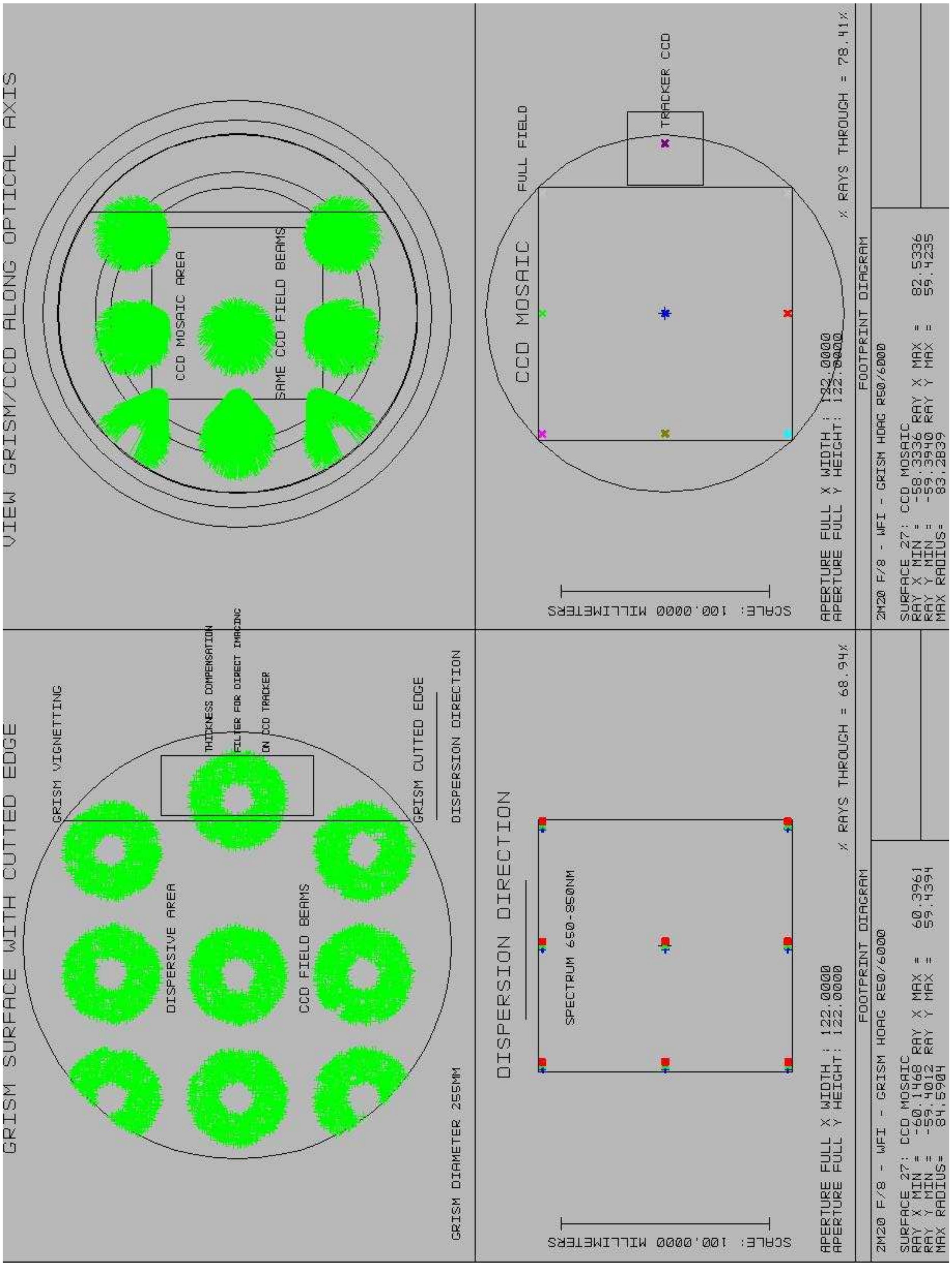

Figure 6: The field of view covered by the grisms is shown in four different presentations: Top left: The (circular) field of view of the optics projected onto the the grism. Pupil images of point sources at various locations appear as “donuts”. Note the vignetting of the sources in all four corners. The vertical line to the left of the tracker CCD marks the edge along which the, otherwise circular, grism is cut. A piece of glass inserted here compensates for a difference in focus between the tracker CCD and the science mosaic. Top right: A view along the optical axis from the grism to the mosaic. Bottom left: The location on the mosaic of the first order spectra of the 8 stars shown in the upper two panels. Each pair of points corresponds to wavelengths 650 and 850 nm, respectively. Wavelength increases from left to right.

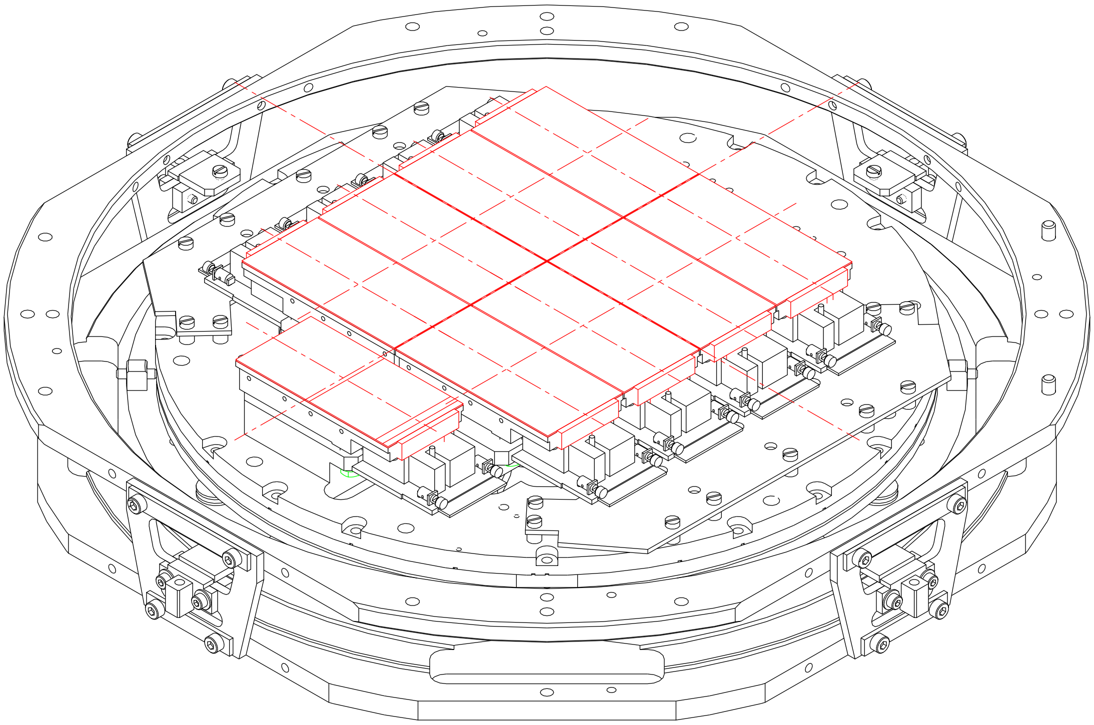

Figure 7: Layout of the mechanics of the detector head, i.e., cables, electronics boards, entrance window, etc. are not shown. The eight rectangles form the science mosaic (Sect. 2.5.1), the additional one on the left is the tracker chip used for autoguiding (Sect. 2.5.2). For the orientation on the sky and the numbering scheme of the CCD's see Fig. 4

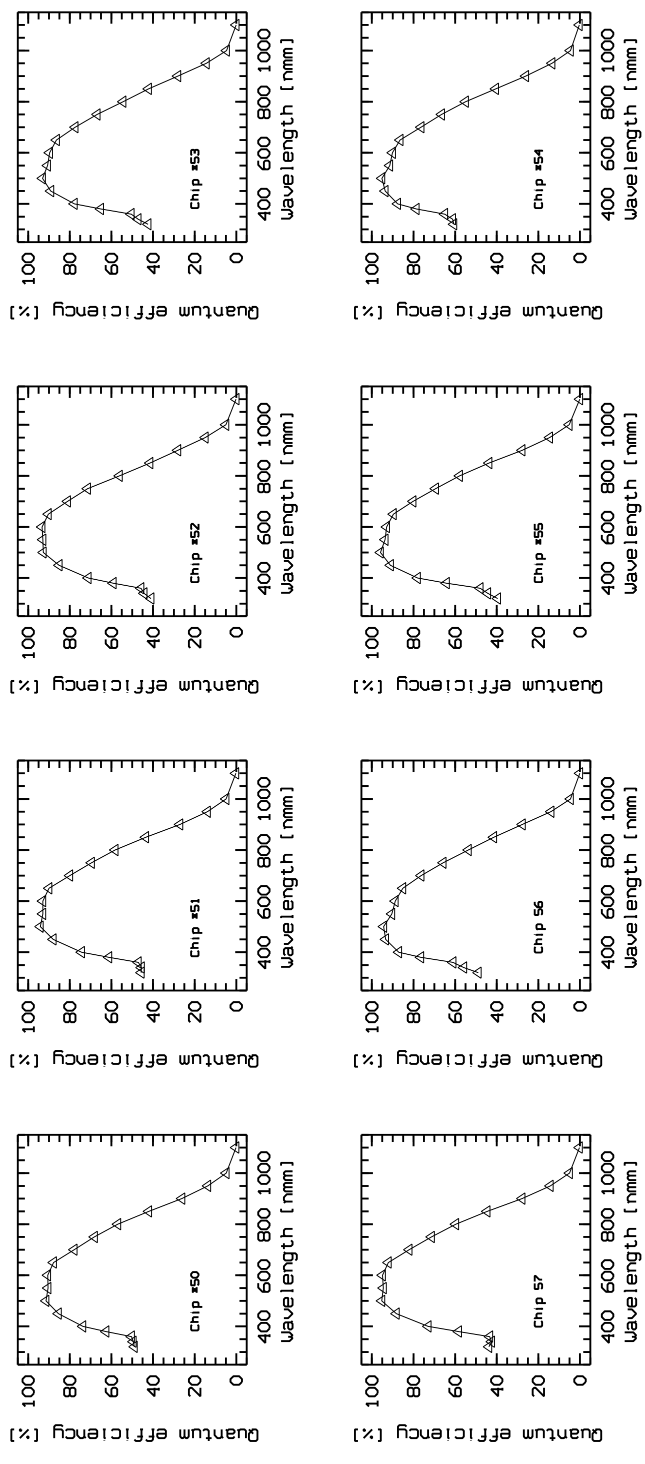

Figure 8: The quantum efficiency of the 8 chips in the mosaic as measured in the laboratory; owing to a possible small problem with the absolute calibration, the QE figures may have to be scaled down by a factor of 0.05-0.1 which, however, is the same for all chips. The numbering scheme is the same as in Fig. 4

Of the two readout ports per chip (in the mosaic they are on the 'outer' short sides - Fig. 7) only the one with the better noise characteristics is used. The readout ports are not selectable by the user. The readout speed is fixed at 357,000 pixels/port/s which corresponds to a readout time of 27 seconds. The overhead for the creation of the FITS file, the data transfer to the workstation, and the display on the Real Time Display together take another half minute. For most purposes, the read noise of around 5 e^-/pixel (cf. the following table) should be practically negligible in comparison with the photon shot noise of the sky background.

	CCD #50	CCD #51	CCD #52	CCD #53
Read noise [ADU]	2.3	2.3	2.1	2.3
Gain [e^-/ADU]	1.9	2.0	2.2	1.9
Read noise [e^-]	4.5	4.6	4.6	4.4
	CCD #57	CCD #56	CCD #55	CCD #54
Read noise [ADU]	2.1	2.2	2.4	2.4
Gain [e^-/ADU]	2.1	2.1	1.9	1.9
Read noise [e^-]	4.5	4.6	4.7	4.5

For instance, even during a dark night, a B-band exposure needs to be shorter than 2 minutes in order not to be sky-noise dominated. The exposure time calculator (Sect. 4.2.1) can be used for the evaluation of more specific cases. Upon readout, the data are written directly to the Real Time Display (Sect. 5.13.1) for immediate inspection.

Note the good match between read noise and gain so that the contribution by the A/D conversion to the noise is negligible whereas the dynamical range of the CCD is optimally exploited.

The charge transfer efficiency is better than 0.999999 in both parallel and serial direction. This means that of the charges in the pixel diagonally opposite of the readout port (from where the charges have to be shifted the largest number of times before they reach the readout port) a fraction of $0.999999^{4098} * 0.999999^{2046} = 0.996$ still appears in exactly that pixel of the image. The remainder is smeared out to subsequent pixels.

The dark signal is hardly measurable and typically of the order of 0.3×10^{-3} to 0.6×10^{-3} ADU/sec/pixel.

The following on-chip binning patterns are supported: 1×1, 2×2, 3×3, 1×2, and 1×3. The latter two are intended to be used with spectroscopic applications (Sect. 2.3) if the spectral resolution is not to be reduced by binning. Windowing of the mosaic is not offered, i.e. only the entire mosaic can be read out. The only exception are focus exposures which only utilize the chip in position 'a' (Fig. 4).

2.5.1.2 Other properties

The physical saturation limit is more than 200,000 e^- per pixel. At the fixed inverse gain factor, which varies between 1.9 and 2.2 e^- from CCD to CCD (see table below), the 16-bit A/D converter provides a dynamical range up to roughly 130,000 e^-. Over this range, peak-to-peak deviations from linearity range from 0.2 to 0.8%, in the case of CCD #55 to 1.6% (Fig. 9). Currently available evidence suggests that the nonlinearity is extremely stable so that the data can be reliably corrected for it.

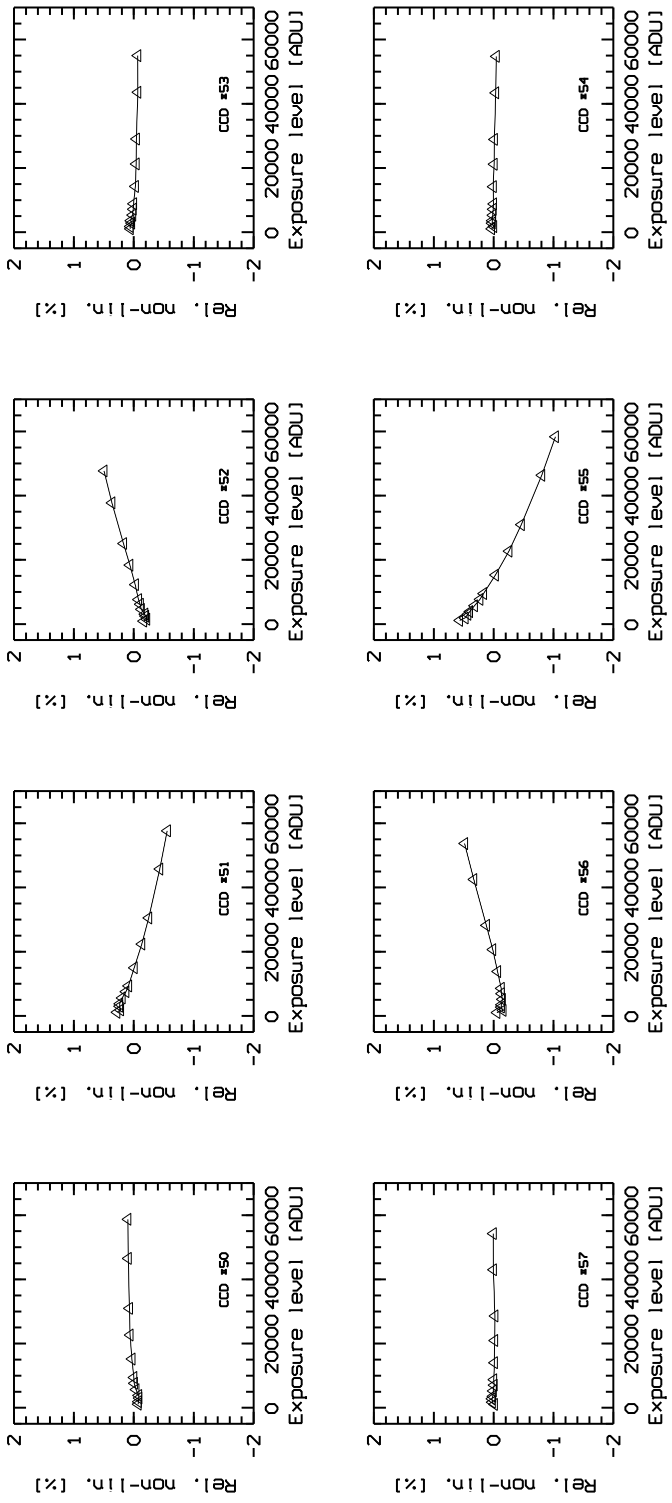

Figure 9: Deviation (in percent) from perfect linearity as a function of the exposure level. For instance, if an exposure with CCD #55 in some pixel reaches a level of 60,000 ADU's, it is actually too low by about 600 ADU's (i.e., by 1%)

Strong overexposures lead to charge overflow ("blooming"). The number of vertically adjacent pixels affected by this depends on the overexposure factor with respect to the saturation level of the A/D converter at 130,000 e^-/pixel (physically, it is the overflow of the saturation limit of the pixel but directly measurable is only the saturation of the A/D converter) and the direction with respect to the readout port. The following table gives a crude indication of the order of magnitude for point sources. ℓ_1 denotes the number of pixels concerned towards the readout port, ℓ_2 the one in the opposite direction (note that on the southern group of CCD's [cf. Fig. 4] the ports are at the southern edge and on the northern group at the northern edge):

Direction	Overexposure factor							
	2	4	5.8	10	25	50	100	1000
ℓ_1 [pixels]	0	0	1	2	8	19	39	344
ℓ_2 [pixels]	0	0	1	3	5	8	13	136

Another side effect of strong saturation can be signal remanence. It is primarily due to electrons generated at the surface of the CCD where they are only weakly exposed to the electrical field applied to read the CCD. Since they can, therefore, only be removed after diffusion has let them drift into deeper layers, reading or wiping the CCD is not necessarily very effective to remove remnant charges. It is the diffusion time which sets the pace. However, the laboratory and commissioning test data described below to check for cross talk did not yield any detectable remnant signal in immediately subsequent (but short) dark exposures.

Because the CCD's in the mosaic share various components of the control electronic, it is, in principle, possible that some cross talk occurs as the result of which a strong signal in one CCD would lead to a weak "echo" in the data coming from one or more of the other CCD's. Laboratory measurements with only a single small light spot, which was integrated on such as to exceed the physical saturation limit by a considerable factor, showed a very weak measurable remnant signal only in very few combinations of exposed and not exposed CCD's. The level of this electronic ghost of less than 5 ADU's should for most practical purposes be negligible. In fact, 15-second integrations on an isolated 4th magnitude star did not detect any electronic ghosts at all.

Since there will often be bright stars in WFI fields, users may nevertheless wish to watch out for this effect. As it only occurs in case of heavy saturation, electronic ghosts can be easily distinguished from real objects by the presence also of the charge overflow pattern as in the real image. The readout timing of the mosaic would suggest that the most likely areas to be affected are those with the same pixel numbers *relative to the respective readout port*. That is, the different readout directions of the two rows of CCD's in the mosaic as well as the fact, that chip #57 is read out in the direction opposite to the other chips in that row, need to be kept in mind.

Tables 7+8 and 9 lists column numbers and their starting rows of all hot and dark columns, respectively. Note that, because of the opposite read-out direction, for chips #54 through #57 (cf. Fig. 4) defective columns extend from their starting point towards higher row numbers whereas for chips #50 - #53 they affect rows with lower numbers. Note further that, as a result of the photographic definition of the pixels through a mask of 1024×512 pixels, which is offset twice in the horizontal direction and in 8 steps along the other axis to cover the entire chip (this process is sometimes called 'stitching'), the central column and every 512th row appear in a flat field exposure either brighter or darker than the others. This is not a chip defect but simply due to such columns and rows being very slightly broader/narrower than the others so that they are exposed to more/less light than on average.

Other cosmetic defects are:

CCD #50: In the area between columns Nos. 900 through 1250 and rows Nos. 2930 to 3160, this

CCD has a number of hot pixels. Most of them are aligned along an arc and are also the starting point of hot columns.

CCD #52: There is a scratch between columns Nos. 1560 and 1760 which extends from row No. 3770 to No. 4098.

CCD #56: Rows Nos. 3589, 3797-3707, and 3779-3781 are partly or over their length dark.

All CCD's: Numerous low-sensitivity pixels, both single and in small clusters. They flatfield out at a level of 0.5% or better.

The charged-particle hit rate at levels above 200 ADU's, where the contribution of imperfectly subtracted bad pixels becomes negligible, is between $0.15\,10^{-6}$ and $0.3\,10^{-6}$ pixel^{-1} sec^{-1}.

Further information incl. reports on the most recent tests can be found on the WWW pages of the 2.2-m Telescope Team (URL: http://www.ls.eso.org/lasilla/Telescopes/2p2T/2p2T.html) and ESO's Optical Detector Team (URL: http://www.eso.org/odt/).

2.5.2 The Tracker Chip

On the eastern side (on the sky) of the science mosaic, there is one additional 2k $\times$ 4k detector (cf. Fig. 7). It is of the same type as the science CCD's but the lower two thirds of the ~500 columns farthest from the mosaic are strongly compromised by numerous cosmetic defects. The practical impact is low, though, because this part of the chip is also the strongest vignetted by the mount of the camera optics (cf. Fig. 4). Further vignetting occurs on the side by the filter holder. The fully useful area is roughly banana-shaped and extends over columns Nos. 800-1880 (counted from the East) of the detector. If a bright enough guide star is available outside this central strip, it can be used without restriction. If a choice is possible, remember that differential atmospheric effects between guide star and mosaic are minimized when the distance (and the difference in airmass!) between the two is smallest.

For autoguiding, a small sub-window of typically 50×50 pixels (maximum: 200×200) centered on the guide star is used. Because the tracker CCD and the science mosaic share the same shutter, the charges are, at a rate of 40,000 lines/s, very rapidly shifted towards the 'bottom' of the CCD until the window in question is fully hidden behind a mask, where it can no longer be contaminated by light. The high speed also ensures negligible trailing of the images. Once under the mask, the window is read out at a speed yielding suitable noise characteristics. The maximum rate is about 1 Hz. The default integration time is 2 seconds. For fainter stars it can be increased. However, because of the periodic 240-sec error of the telescope's alpha drive (Sect. 2.6.2), it is not advisable to user longer integration times than necessary.

For guide star acquisition purposes, acquisition exposures can also be made. In this mode, the full CCD is read out within ~15 s; the image cannot be saved to disk.

A baffle between tracker chip and science mosaic shields the latter against stray light from bright guide stars (but see Sect. 2.8).

The practical usage of this chip for autoguiding (and other purposes) is described in Sect. 2.6.3.

2.6 The 2.2-m Telescope

2.6.1 Optics and Image Quality

The MPG/ESO telescope is of a Ritchey-Chretien design with an f/8 Cassegrain focus. Except for the missing coudé focus, it is basically a twin of the 2.2-m telescope at the German-Spanish Observatory on Calar Alto, Spain. In 1998, it was subjected to a comprehensive overhaul and refurbishment of its mechanics and control electronics which accomplished considerable improvements in performance. Detailed optical tests have confirmed its excellent optical quality. The total (quadratic) contribution by its intrinsic optical aberrations to the image size does not exceed 0.35 arcsec. For most practical purposes this is negligible. More detrimental can be heat sources and insufficient ventilation of the dome. Near-IR mages of 0.6 arcsec FWHM have been obtained during the WFI commissioning.

The dome follows the telescope automatically. One moveable upper and lower windscreen each are installed to shield the telescope against wind shake but not yet operational.

2.6.2 Pointing and Tracking

The primary pointing model is established for a reference pixel on the tracker CCD with which the measurements are made. However, for normal observations, offsets are automatically applied so that the field center specified appears about 15 arcseconds west and south of the northeastern corner of chip position “e” (cf. Fig. 4).

The pointing model provides an accuracy of 5-10 arcsec (rms) over the range from 0 to 60 degrees in zenith distance. Offsets up to 3 arcmin have an absolute accuracy of ±0.5 arcsec and are reproducible to within ±0.2 arcsec.

Pointing limitations: The zenith distance must be lower than 70 degrees. (But note that at so large zenith distances pointing and tracking are inferior).

Free tracking quality: There is periodic error in the alpha drive mechanics with a period of 240 sec and peak-to-peak amplitude of 1.2 arcsec. Over 16 minutes, i.e. a multiple of this period, the free tracking was measured to be accurate to slightly more than 1 arcsec. Usage of the autoguider (Sect. 2.6.3) improves the performance to better than 0.1 arcsec.

2.6.3 Autoguiding

Autoguiding is only done in (and only requires) a small window of the tracker CCD (Sect. 2.5.2). Only for the selection or for the confirmation of the identification of a guide star is the full frame displayed on a separate incarnation of the Real Time Display (Sect. 5.13.1). These steps are performed by the telescope operator.

When the telescope is offset in order to cover the gaps between the CCD’s in the mosaic, the window on the tracker CCD can be automatically offset by the same amount so that autoguiding can continue with re-identification of the guide star. This is known as combined offsets.

It is not necessary to select guide stars in advance as this is done in real time at the telescope (Sect. 4.2.3). However, if you want to take advantage of the possibility of an automatic absolute astrometric calibration (Sect. 2.9.4) of your frames, read in Sect. 4.2.3 how this relates to the centering of the science targets in the science mosaic.

The autoguider can also be used to monitor the telescope tracking and *variations* of the point spread function (PSF) and the sky transparency (Sect. 5.12.1). A corresponding graphical display is available. <u>Note</u> that the FWHM is *not* representative of the absolute image quality in the mosaic because the tracker CCD is rather far from the plane of the latter so that guide star images are significantly out of focus when the telescope is properly focussed on the mosaic. Moreover, the imaging quality of the auxiliary filters is quite limited.

Because guide stars have a range of colours and they are observed through different filters (Sect. 2.2.2), only an approximate limiting magnitude can be given above which stars can no longer be used for autoguiding. It is around 16-17 mag. Note that this limit depends on sky brightness, seeing, integration time, and wavelength. Normally, there is not even at high Galactic latitudes a problem to find a guide star of sufficient brightness, especially if the degree of freedom afforded by the wide FOV is exploited to slightly offset the telescope from the nominal coordinates.

Since tracker CCD and science mosaic share the same shutter, the shutter is briefly closed after autoguiding has started, and the CCD's of the mosaic are wiped a few times. Then, the shutter opens agains, the science exposure starts, and autoguiding is resumed. All this is taken care of automatically by the TCS and DAISY+ and, therefore, completely transparent to the user.

Differential autoguiding over distances not exceeding the useful field of view of the tracker CCD (Sect. 2.5.2) is fully supported.

2.6.4 Finder Telescope

Because of the large field of view of the instrument and the short read-out time of less than 30 seconds, remote access from the control room to a finder telescope is not offered.

2.7 Limiting Magnitudes

An approximate graphical presentation is provided in Fig. 10. More specific and precise estimates are possible with the exposure time calculator (Sect. 4.2.1).

2.8 Known Imperfections and Deficiencies

Nothing is perfect and neither is the Wide Field Imager. Depending on their requirements, users may wish to carefully consider the following points (a more extensive and continually updated list is maintained in the form of *A Practical Guideline for WFI Observers* which can be copied from the WFI WWW home page mentioned in Sect. 1.1):

Bias variation: After each (re-)start of an observing session, the bias values can differ from the previous ones by a few ADU's. When the CCD's have been idling for some time, it is recommended to take a few bias exposures before taking any calibration or science exposures so that the system can reach equilibrium. Thereafter, bias values should remain constant. Chip-to-chip differences in bias value are normal as the offsets can be fine-tuned only imperfectly.

Bias from overscan pixels: Because of this variability, it is often best to use the bias values in the overscan pixels. Because of the finite response time of the control electronics, the bias level can depend on the signal level in the corresponding light-sensitive part of the row. This can be seen in flat field exposures where the bias value increases over a few hundred rows asymptotically from the row closest to the readout port.

Stray light from the tracker: In spite of shielding, light of a bright star falling onto the tracker CCD can be reflected onto the science mosaic. A similar effect is seen in flat field exposures through filters with an auxiliary filter for the tracker. Because the bandwidth of the auxiliary filter is usually larger (in the case of medium- and especially narrow-band filter: very much larger) than the one of the main filter, the excess light partly scatters onto the mosaic. This is visible as a band of enhanced brightness along the height of the tracker CCD.

Vignetting by filter holders: On some interference filters the optically active coating does not quite extend over the full size of the filter. In order to avoid contaminating unfiltered light, the edges of such filters have been masked off by the filter holder. This appears as a slight vignetting over the outermost couple of hundred pixels.

Vignetting by the Rc filter: The Rc filter is circular (rather than square) and as a result, the images are slightly vignetted at the corners.]

Light scattering by filter holders or dewar entrance window: When a bright star is positioned just outside the field of view it creates a strong light "fountain" of scattered light. The light pours in at a right angle with respect to the edge of the field. It is visible when the star is within the first 90 arcsec outside the directly observable field. With about 300 arcsec length, the beam of scattered light reaches it largest extent when the star is about 60 arcsec outside the field. If such a situation arises, the best remedy is to place the disturbing star at least 100 arcsec outside the FOV. Putting it within the FOV can still be the next best solution.

Optical ghosts: Very bright sources lead to the appearance of two images of the pupil on the diagonally opposite side of, and at about the same and twice the distance from, the center of the FOV. For a direct image saturating the A/D converter a few hundred times, the first ghost reaches a level of a few tens of ADU per pixel; the second one half that much. The first one measures about 100 arcsec, the second one 200 arsec in diameter.

Heavy saturation: Without binning, the amplifier can no longer cope with the charges once about 40-fold saturation of the A/D converter is reached, and the pixels concerned suddenly turn 'black'. This point is reached very much earlier with 2×2 and especially 3×3 binning.

Delayed closure of shutter: In very few cases it has been noticed that the shutter closed only after readout of the CCD had started. The give-away symptom is that the images of all sources, faint or bright, have slightly wiggly tails towards the central East-West symmetry axis of the mosaic. This is not be confused with charge overflow which only occurs with strongly overexposed pixels and always follows a perfectly straight line (namely CCD rows). From the very small numbers of cases observed, it seems that this problem occurs preferrentially with exposure times below 2 seconds.

Dewar temperature and cosmetic defects: Laboratory tests with the WFI CCD's in a single-chip dewar have shown that at temperatures 10-15 degrees below the WFI operating temperature of 169 K, more cosmetic defects freeze out at almost no loss in sensitivity. At least as important is that the operating temperature is stable. This is the case. But although all possible efforts were made, the large size of the dewar entrance window and the thermal leakage associated with it did not permit a safe, lower operating temperature to be set.

Astigmatism: At the time of writing, the telescope suffers significant astigmatism outside the circum-zenithal region, especially at positive hour angles. This leads to an elongation of stellar images by typically 0.5 to 1 pixels. When the difference between the current position of the telescope and the one, where the last focus sequence was made, exceeds $\sim$30 degrees, a new focus sequence is advisable.

Especially at large zenith distances it can happen that the filter exchange mechanism really fails or only erroneously detects a malfunction. The recipe to correct this problem is known to the telescope operators.

2.9 Calibrations*

ESO distinguishes between the calibration of an instrument and the calibration of a set of observations. The instrument calibration is the responsibility of the Observatory which makes the corresponding calibration relations available to the users. This is described in the WFI Calibrations Plan [1]. In most cases ESO will also offer the tools needed to apply these calibrations to the scientific data (TBC).

The instrument calibrations are done in calibration and maintenance nights which are combined with periods of service observations (Sect. 3.2). The time is not charged to the programmes that could benefit from them. However, if there are long periods without service observing so that calibrations might become invalid, the Observatory reserves the right to use up to 10% (TBC) of the time assigned to a visitor for such calibrations. The 2.2-m Telescope Team Coordinator will carefully assess how this can be done with a minimum of impact on the observing programmes.

This section describes only briefly what is calibrated and to what level of accuracy. Observers wishing to make their own calibration exposures may find Sect. 4.3 useful. Sect. 6 deals with the application of the calibrations to the scientific data.

All calibration data are kept in the Calibration Database (Sect. 6.3).

2.9.1 Photometry*

Regular calibrations are maintained for the `U/360, B/99, B/NEW, V/89, Rc/162 and Ic/Iwp` bands only. Their zeropoints can be found at:
http://www.ls.eso.org/lasilla/Telescopes/2p2T/E2p2M/WFI/zeropoints/
The CCD pixels are not binned. The primary calibration quantity is the overall (telescope-to-detector) system response in units of e^- / erg (TBC). Using this quantity, the pixel size of 0.238 arcsec (TBC), and the exposure time, the number of electrons detected in a pixel can be easily converted into surface brightness at the telescope entrance. If the colour of the target is known, the first-order colour coefficients of the transformation can be additionally used, which are also supplied. (Calibrated data delivered to the applicants are, of course, also corrected for the mean atmospheric extinction.)

The uncertainty of the calibrated system response is TBD% in all filters mentioned.

2.9.2 Spectroscopy*

For both grisms (Sect. 2.3), a dispersion relation is available with a typical accuracy of TBD pixels. Since there is no slit so that comparison spectra cannot be taken, the zero point has to be inferred from the image of the zeroth spectral order of each source which, owing to the prismatic properties of a grism, is elongated with an aspect ratio of about 2-3, depending on the seeing. Other suitable fiducial marks, especially for extended sources, may be spectral features in the object (if the redshift is negligible), telluric absorption lines, edges of wavelength-range limiting filters, or astrometric transfers from direct images. With respect to the latter, note that observations with and without grism or with different grisms cannot be carried out within one night because the entire instrument has to be taken off the telescope in order to mount or dismount a grism (Sect. 2.3).

Spectrophotometric or spectropolarimetric calibrations are not offered.

2.9.3 Polarimetry*

Polarimetric calibrations do not currently form part of ESO's calibration efforts for the WFI. All calibrations need to be planned and executed by the applicants.

2.9.4 Astrometry*

If a guide star with known coordinates is used (Sect. 4.2.3), the astrometry relative to these coordinates is better than 3 arcsec (TBC).

The maximum variation in plate scale over the field of view is 0.08 % (TBC). A master distortion map is available.

For observations taken in connection with an approved observing programme with other ESO instruments that require high-precision astrometry, a special procedure yields a *relative* accuracy of 0.15 arcsec (rms).

2.10 Data Products*

Visiting Observers (Sect. 3.1) may copy any calibration data (Sect. 6.3) and any of their observations to DLT or DAT (Sect. 5.15). Additionally, *all* users of the WFI will receive a set of TBD media with the following:

- An excerpt of the log files (in ASCII format TBC) from the Meteorological Monitoring System (Sect. 5.12.2) and the autoguider (Sect. 5.12.1)
- The raw frames in FITS format (Sect. A.10.1)
- All pertinent archival calibration data (Sect. 6.3), if any, in FITS format (Sect. A.10.2)
- If applicable (Sect. 6.2) the pipeline-processed, calibrated data in FITS format (Sect. A.10.3)
- An ASCII-format table of contents which, where applicable, relates raw frames, reduced frames, and the relevant calibration data to the Observation Blocks (Sect. 4.1.2) the execution of which generated the raw frames. For all frames there are flags which encode the results of the quality check (Sect. 6.1).

3 Operating Modes*

The operations paradigm adopted for the 2.2-m telescope and its presently only instrument, the WFI, was inspired by the VLT operations model, which at La Silla has been proto-typed and tested with the NTT. However, it has been simplified and de-scoped as to be commensurate with the comparatively much smaller value of the facility. Furthermore, the La Silla Observatory will gradually test this new operations paradigm also with its other telescopes. Depending on the experiences made with these other telescopes, also the one in use for the WFI will evolve with time. The projected ultimate operations scheme is outlined in the WFI Operations Plan [2].

This evolution bears the risk of mistakes for which we ask in advance for your patience. But it also offers users the opportunity to provide effective feedback which we would like to encourage again (cf. Sect. 1.2).

There are four major changes with respect to the traditional operations scheme at La Silla:

Service observing: Depending on the possibilities of the applicants and the requirements of their observing programmes, applicants may request that their observations be performed in their absence by ESO staff. This is described in Sect. 3.2.

Observing Templates: In order to provide a solid platform for service observations, that minimizes the risk of mutual miscomprehensions, ESO offers a fixed menu of standard observing patterns. These so-called Observing Templates are the subject of Sect. 4.1.1.

Instrument calibrations: For the scientific observing templates, ESO will maintain a range of calibrations (Sect. 2.9) for which dedicated technical time will be used. Their primary purpose is to support a continuous quality control (Sect. 6.1) of the essential instrument performance parameters. To within the stated uncertainties, they are also useful to calibrate data obtained with standard observing templates. Only if a higher precision is required, will applicants have to perform/specify their own calibration observations. The time needed for such extra calibrations will have to be covered by the total time allocated to the observing program concerned.

Pipeline data reduction: With standard observing patterns and observatory-maintained instrument calibrations, the observatory can not only provide the facilities to gather observations and deliver the raw data but also apply some basic calibrations to remove the main instrumental signatures. For a summary of the description of the pipeline reduction process see Sect. 2.10.

All observational data will be supplemented with extensive ancillary information (Sect. A.10.3) and be kept in the ESO Archive (Sect. 7). Usually, all data will be protected by a proprietary period of one year starting after the delivery of the last data to the applicants. Calibration data will not be protected.

3.1 Visitor Mode

Observers will usually arrive at least one, preferrably two, days before the observations start. They will meet with their Introducing Astronomer to clarify any questions, which the reading of this manual still has left open, and to further prepare their observations. It is also a good practice to ask the respective previous observer for permission to visit them at the telescope. Finally, the problem report database can be a valuable in-advance source of information about persistent or recurrent anomalies (in spite of all efforts: occasionally they do exist). In the first night, the Introducing Astronomer will stay with the observers until they have acquired sufficient operating knowledge.

At the telescope, ‘visitor mode’ means the following:

- Observers edit Observing Template signature files (Sect. 4.1.1) and create Observation Blocks (Sect. 4.1.2). If necessary for a given programme, this includes calibration exposures. Normally, this is done well ahead of time. But the capability to create new or edit existing OB's is provided.
- The telescope is operated (focussing, pointing, offsetting, guide star selection, supervision of guiding, etc.) by the telescope operator.
- The dome is operated by the telescope operator.
- The operator is responsible for the safety of the equipment and its users. If the need arises, e.g. because of bad weather, (s)he will suspend the observations.
- Fields are identified by the observer.
- The execution of Observation Blocks is planned, started and supervised by the observer.
- The observer is responsible for quality control (Sect. 6.1).
- At the end of the night, operator and observer prepare the daily operations report (Sect. 5.16).

The telescope operator can also help with the preparation of calibration exposures. However, their execution is the responsibility of the observer. In particular, lengthy sequences of dome or twilight flat-field exposures are not covered by the working hours of the operators.

Note that the observatory maintains a Calibration Plan [1] for the WFI. ESO makes every effort to minimize the impact of its execution on observing runs performed in visitor mode. However, in order to maintain continuity of the calibrations, ESO reserves the right to use up to 10% of any night to execute calibrations demanded by the calibration schedule. The Introducing Astronomer will inform visitors at the beginning of their run whether and when such calibrations are foreseen.

3.2 Service Mode*

In this mode, applicants fill in template signature files (Sect. 4.1.1) and build Observation Blocks (Sect. 4.1.2) after they have been notified of observing time granted to their proposals. The letter of notification will also state where template forms and instructions can be obtained and by when the filled-in forms have to be submitted. Usually, the deadline is one month before the beginning of the observing semester.

3.2.1 Scheduling*

The scheduling takes into account the visibility of the targets, the rating given to the programme by the Observing Programmes Committee, any absolute timing requirements, and the priority assigned to each Observing Block by the applicants. These latter priorities are effective only within a given programme. In order to make an observing programme easily schedulable, it is essential that applicants oversubscribe the time allocated to them by a factor of 2 (but not more than 3). However, once the number of hours granted to a programme has been reached, its execution is terminated. The scheduling process gives some preference to completing programmes which are already well advanced rather than starting new ones. Observation Blocks that can share calibration data are preferrentially grouped together.

Users can specify scheduling constraints, namely absolute time (to within TBD minutes), time relative to some other event/action (to within TBD minutes), phase of the moon, sky transparency, and external seeing. However, they need to be aware that the more constraints are set, the more this reduces the probability that they are fulfilled simultaneously and that the observation can be executed. In service mode (Sect. 3.2), absolute times not falling into the service observing periods announced in the call for proposals can for obvious reasons not be accepted.

3.2.2 Execution of Observations*

All observations are executed *as specified by the users.* Only if very obvious errors seem to be in the exposure definitions, may ESO contact the applicants and request a confirmation or correction.

ESO only endeavours to comply with the user specifications for the observations and to ensure the nominal performance of the equipment. If the data are nevertheless not useful for the aimed-at scientific purposes, ESO does not accept responsibility for this.

4 Preparing the Observations

This section describes the technical steps of the preparation of an observing run. Observations can only be defined by editing Observing Template signature files (Sect. 4.1.1) and creating Observation Blocks (Sect. 4.1.2). A variety of tools and advice that may be useful in doing so are described in Sect. 4.2.

Early and careful assessment of the calibration needs is important for every observing program. Sects. 2.9 and 4.3 expand on considerations that may be worth taking into account.

For visitor-mode programmes (Sect. 3.1) it is advisable to prioritize the individual exposures to be made and for each night to think about the order in which they are to be executed. Unless there are any absolute timing requirements, exposures should be taken as close to the meridian as possible. This minimizes atmospheric effects (extinction, seeing, refraction, etc.) in an absolute sense. But over the large FOV of the WFI also differential effects become noticeable at large zenith distances. Although in the case of refraction only its second derivative with respect to zenith matters, it can in the extreme case of an exposure covering the range from 50 to 60 degress in zenith distance reach 1 arcsec.

A list of Landolt photometric standard stars and associated finding charts is posted on the Web page: http://www.ls.eso.org/lasilla/Telescopes/2p2T/Landolt/Landolt.htm

Owing to the large FOV, finding charts should not normally be required. But the Digitized Sky Survey (URL: http://archive.eso.org/dss/dss) can be useful to check for the presence of disturbing bright stars. Day- and moonlight tables for La Silla (URL: http://www.ls.eso.org/lasilla/Sun-Moon/Sun-Moon.html) are also available on the Web.

In service mode (Sect. 3.2), preparing the schedule is not the applicant's task. But by facilitating the schedule building (Sect. 3.2.1), the probability that a programme is completely executed can be significantly increased.

For each exposure, the following and only the following parameters can be defined by the user

- an ASCII identifier (no default)
- the filter (no default) - Sect. 2.2.2
- the detector binning (default: no binning) - Sect. 4.2.4
- the exposure time (in seconds, no default)
- the equatorial coordinates (no default)
- the epoch (default: J2000.0)
- the tolerance for the off-centering of the nominal coordinates (default: 120 arcsec) - Sect. 4.2.3
- the tracking rates (default: sidereal tracking, i.e. target not moving)

Observing Templates (Sect. 4.1.1) have their own, additional operations parameters associated with them.

Furthermore, scheduling constraints (Sect. 3.2.1) can be set:

- absolute time
- time relative to some other event/action
- phase of the moon
- sky transparency
- external seeing

4.1 Defining Observations*

The only building block of an observing program that the control system for the WFI handles (Sect. 5.10) are the so-called Observation Blocks (Sect. 4.1.2). However, Observation Blocks may have an internal structure; these "sub-atomic" strutures are the Observing Templates (Sect. 4.1.1). The latter can only be single or multiple exposures; multiple exposures must be identical except for the starting times and telescope offsets. The sole purpose of the Observation Blocks is to enable the user to ensure that groups of exposures that only make sense if they are complete, are scheduled and executed together. If the user does not wish to link multiple exposures together, an observing programme could consist entirely of Observation Blocks each of which includes only one single-exposure Observing Template. The WFI does not support a high-level command language such as the Sequencer of the VLT.

Off-line preparation and submission: TBD

4.1.1 Observing Templates*

To each Observing Template belongs an Observing Template signature file. The user edits the associated form (details and source: TBD) which lists and explains all user-defineable parameters. Where defaults exist, they are inserted and marked as such but can be overwritten. The template signature files are ASCII files so that also any text editor can be used to create them. Only the structuring and naming conventions must be followed; examples can be obtained from TBD.

Within a single template signature file, only one value per parameter can be specified. For instance, observations of the same field but through n different filters require n template signature files (which, however, may be combined into one Observation Block: see Sect. 4.1.2). But multiple exposures of the same field with the same filter are possible within a single template signature file.

The number, scope, and diversity of templates will evolve with time. At present, the following templates are supported:

Generic: Any user-defineable WFI parameter (see above) can be set to any supported value. The telescope will work in stare mode only (cf. below).

The purpose of this template is to deliver the full, unconstrained technical capability of the WFI to the user. However, its usage is recommended only if other templates do not offer the required functionality. Observations resulting from the `generic` template cannot be processed by the pipeline even if the `generic` template were used to emulate other templates.

Stare: One or more exposures at the same telescope position, with the same exposure time, and through the same filter can be defined.

Dither: Same as stare mode except that between the exposures the telescope will be moved from the reference position by small offsets.

The values of the offsets in RA and DEC (both in arcsec and always *relative to the reference position*) are the only additional parameters.

This is the recommended default template for all imaging, spectroscopic, and polarimetric observations. If during the data reduction the exposures are combined into one image, detector blemishes, particle hits, and the gaps between the CCD's in the mosaic (Sect. 2.5.1) can be removed. Note that, because of the presence of horizontal *and* vertical gaps, the minimum number of exposures needs to be 5. Only then will all parts of the field be covered by the conventional minimum of 3 exposures that permits detector defects and particle events to be corrected for. But a larger number is recommended, if the readout noise does not disturb. The offsets have to be large enough to fully cover the inter-chip gaps but should be kept sufficiently small so that the need to change guide stars (Sect. 2.5.2 and 4.2.3) between exposures is not likely to arise. Instead of specifiying individual offsets, users may also select a default offset pattern that aims at satisfying all constraints in an optimal way. In the absence of project-specific requirements, its usage is recommended.

Bias: The user can specify: number of readout and CCD binning factors.

Twilight flats: The user can specify: base exposure time or exposure level, filter, number of readouts, and CCD binning factors. DAISY+ (Sect. 5.3) sets the base exposure time at run time, if it has been defaulted, and during the sequence steps it up or down as appropriate.

Dome flats: The user can specify: exposure time or exposure level, filter, number of readouts, and CCD binning factors.

Photometric calibration: There is an on-line catalog of fields with photometric standards (Sect. A.7) but the user can also observe any other field. The user can specify: field name or coordinates, pointing tolerance, exposure time, filter, number of readouts, and CCD binning factors. For filters to which the tabulated magnitudes and colours of the catalog fields are applicable, field name, pointing tolerance, and exposure time can be defaulted. In this case, DAISY+ chooses the most suitable field at run time and sets the exposure time accordingly.

Spectroscopic calibration: There is no specific calibration template.

Polarimetric calibration: The list in Sect. A.8 of fields with polarimetric standards is also maintained on-line, but users may select their own standards. User specifiable parameters are: field name or coordinates, pointing tolerance, exposure time CCD window(s), and the CCD binning factors. If field name and coordinates are defaulted, DAISY+ selects the most suitable one and sets also the exposure time. One calibration always consists of observations through all four filters (Table 3). Since initially there are polarizers for one wavelength range only, the passband is not a free parameter.

Astrometric calibration: There is an on-line catalog of fields with astrometric standards (Sect. A.9). Any other standard field preferred by the user may also be used. The user can specify: field name or coordinates, pointing tolerance, exposure time, and filter. Field name, filter and exposure time can be defaulted in which case DAISY+ chooses the most suitable field and filter at run time and sets the exposure time accordingly. Furthermore, DAISY+ offsets the telescope a number of times and in such a fashion that the resulting set of exposures is suitable for a full astrometric calibration (Sect. 6.4.6).

Note that except for the obvious instrument-mode specific calibrations all three modes, namely direct imaging, polarimetry, and spectroscopy, use the same templates.

For focussing there is a hardwired template built into DAISY+ (Sect. 5.7).

4.1.2 Observation Blocks*

An Observation Block (OB) is an ASCII file which contains the name of one Observing Template signature file per line. No structure (e.g., looping, conditional branching, etc.) other than a straight sequence can be defined. The only user-defineable parameters are scheduling constraints (Sects. 3.2.1 and 4). Logical links between OB's can be defined. All observations within one OB must be of the same field. The naming convention for OB files is TBD. At the telescope, OB's are loaded into 2p2BOB (Sect. 5.9) from where the user can submit them to DAISY+ (Sect. 5.3) for execution.

After a couple of consistency checks, DAISY+ carries out the associated exposures one by one until the end of the OB is reached.

Note that it is very advisable to combine only those Observing Template signature files into one OB that need to be executed in an uninterrupted sequence. *If too many exposures are put into one OB, the execution time may become so long that the probability of it being schedulable and/or executable decreases drastically.* An OB is the smallest schedulable and executable unit. If its execution is not possible without interruption, scheduling and execution will not be attempted.

For instance, if the colour variation of pulsating stars is to be observed, the observations through the filters defining the colour should be made at nearly the same time, and one common OB is needed. By contrast, observations of constant objects in different filters can just as well be made even in different nights and should be split into one OB per filter. But the possibility to logically link these OB's (cf. above) should be used in order to signal to the scheduler that only a complete set of such observations of a given field is scientifically useful.

4.2 General Tools and Advice

Note: An additional and continually updated compilation of practical advice is provided on the Web page referenced in Sect. 1.1 as *A Practical Guideline for WFI Observers.*

4.2.1 The Exposure Time Calculator

Because of the necessity to keep the database up to date, the exposure time calculator will be made available on the WWW only (access is provided from the WFI home page given in Sect. 1.1). The layout of the GUI and the on-line help offered therein are sufficient even for first-time users to apply this tool.

User suppliable input parameters are monochromatic magnitude (for point sources) or surface brightness (in erg arcsec^{-2} s^{-1} Å^{-1}, for extended sources), airmass, filter, exposure time, seeing (for point sources), and CCD read mode. The exposure time calculator contributes the instrument database, atmospheric parameters, and the night sky brightness. Output are the number of electrons and the S/N, for point sources per object and for extended sources per pixel. In a second mode, these output parameters are accepted as input and the required exposure times are returned.

As a simple but crude graphical indicator, Fig. 10 shows for a few selected filters the exposure times needed for the 5-σ detection of monochromatic point sources as a function of magnitude.

4.2.2 Operational Overhead Times

For simple, but sometimes subtle, operational reasons, not the entire night can be spent collecting photons. The list below compiles (in alphabetical order) the main overhead times that have to be added to the pure shutter-open times. Where applicable, a full 8 k × 8 k frame is assumed. Additional major tasks running on the computers would increase the times given.

DAISY+ start-up and shut-down: 5 seconds each at beginning and end of a night

Detector readout: 27 seconds

File transfer to instrument control workstation (w2p2ins) workstation and RTD: $\leq$10 seconds (over and above readout time) but significantly increasing when the disk is more than about 80% full

Figure 10: Exposure time (in seconds) as a function of monochromatic magnitude (in several passbands as labeled). The relations shown correspond to 5-σ detections of point sources at a seeing of 1 arcsec and intermediate night sky brightness TBD

File transfer to data reduction workstation (w2p2drs): 45 seconds (after transfer to w2p2ins)

Filter exchange: 2.4 seconds times the difference in position number in the filter storage ring for filter ring rotation plus 45 seconds for the exchange of one filter against the other one (cf. Sect. 2.2)

File saving to DLT: 210 sec (done in background, files are queued)

Reading of FITS file into MIDAS: 50 seconds (done in background)

Filter replacement: daytime (only!)

Focussing: $\leq$10 minutes

Grism insertion or removal: daytime (only!)

Guide star acquisition: $\leq$ 1 minute

Telescope slewing: Over large angles, where acceleration and deceleration times are insignificant, the average speed is about 3000 arcsec/sec.

Parallelism:

1. A new exposure can be defined during execution and readout of the previous exposure. But it can be started only after the readout and data transfer have finished.
2. Similarly, a guide star acquisition image can only be taken after the last science exposure has been completely read out.

3. The telescope can be safely preset to the next field when the file is still being transferred to the instrument workstation. When the file is still being *read*, there is the risk of electromagnetic interference from the dome and telescope drives which would add unwanted noise patterns to the data.

4. The filter can be changed during CCD readout. But, as for dome and telescope drive, additionally induced noise should be watched out for.

5. When defining a new observation requiring a change of filter it is advisable to first select the filter via the corresponding pull-down menu and then press the `APPLY` button. While the filter storage ring turns and the filter is inserted into the beam, all other parameters for the next exposure can be entered and carefully checked. .

6. The reading of the data and the saving to disk are done in parallel. The slower of these two processes is the one that contributes to the overhead (cf. Sect. 4.2.2).

7. The writing to DLT takes place in parallel to all other operations. If new data are generated faster than they can be saved on tape, the files are put in a queue.

4.2.3 Guide Star Selection*

After an Observation Block (OB, Sect. 4.1.2) stored in 2p2BOB (Sect. 5.9) has been submitted to DAISY+ (Sect. 5.3), a suitable guide star can usually be selected automatically by the computer from astrometric catalogs kept on-line. TBC

However, since the tracker CCD (Sect. 2.5.2) is not mounted on a moveable guideprobe, it will at high Galactic latitudes become increasingly less likely that a guide star with well-known coordinates will fall on that chip. Two strategies are possible to overcome this problem:

1. Let the telescope operator interactively select an anonymous guide star that happens to be visible on the tracker CCD. In this case, an automatic astrometric calibration (Sect. 2.9.4) of your image will not always be possible, depending on the crowding of the field and the pointing error of the telescope. However, guesses of the positions of the astrometric standards in the field can be derived from a guess of the telescope pointing so that their manual identification is always possible.

2. Relax the centering requirements for your field on the CCD mosaic. This possibility exists already at the time of definition of the Observation Blocks (Sects. 4.1.2 and 4.1.1). Suppose, you can tolerate that the center of your field may be off the center of the science mosaic by 30 arcsec. If there is an astrometric guide star that falls off the useful area of the tracker CCD by 20 arcsec, permitting an offset of up to 30 arcsec will result in that star becoming accessible for autoguiding.

   If the automatic guide star selector cannot find a star that is compatible with the size and location of the tracker chip as well as with the coordinates of the field to be observed, it will propose an offset so that the nearest guide star can just be used. The user has, then, the possibility of accepting such a modification to the original OB.

<u>Note</u> that for these reasons it is advisable to select the guide star well in advance (off-line) in order not to lose time. Procedure/tools: TBD.

4.2.4 Choosing the Detector Parameters

The only user-selectable parameter is the binning. The available binning patterns are 1×1, 2×2, 3×3, 1×2, and 1×3. The last two are offered for use with the grisms (Sect. 2.3) so that binning is possible without reduction of the spectral resolution.

By binning, any $m \times n$ (m and n integers) pixels can be combined on the chip prior to the readout, so that the read noise would occur only once for the binned, larger pixels. However, the readout noise can already without binning be kept at a very low level. Furthermore, the reduced sampling seriously compromises the spatial resolution (unless the seeing is very poor), and the detectability of particle events is reduced in proportion to the inverse product of m and n. Note that none of the Observatory-supplied calibrations (Sect. 2.9) support binning.

4.3 Calibration Exposures*

The calibration exposures needed for the instrument calibration maintained by the Observatory will be done by ESO staff. The following conjectures are of direct interest only to observers who need their own calibrations. However, since also data reduction aspects are taken into account, observers who cannot depend just on the pipeline-reduced data may wish to continue reading.

4.3.1 De-biassing

In order to avoid the photon and read noise leading to apparently negative numbers of electrons (which would be unphysical), a baseline signal of about 200 ADU's is electronically added to the actual response of the CCD to the infalling light. The amount of this so-called bias can be measured by taking 'exposures' of zero seconds, i.e. by reading out immediately without opening the shutter. It has to be subtracted from all science and calibration exposures. Since the bias level is quite uniform across each chip, subtracting the mean value as a number can often yield better results than subtracting a bias image. If a bias image shall be subtracted, it is necessary to average at least 10 such exposures in order not to add noise to the bias-corrected files.

Remember that the bias level may change after each (re-)start of an observing session with DAISY+ (Sect. 2.8).

Temporal variations of the bias level can be traced by means of the pre- and over-scan pixels (Sect. 2.5.1). There is also a weak dependency of the bias level on the total signal in a row (Sect. 2.8). This, too, can be deduced from the overscan pixels.

4.3.2 Flat-Fielding

Strategy for grism and polarimetric observations: TBD

Flat-field exposures can be useful for alleviating three unwanted effects in the raw data: (i) pixel-to-pixel sensitivity variations of the detectors, (ii) interference fringing in the detectors, and (iii) large-scale illumination inhomogeneities. In the WFI all three sources of quality degradation are weak but the improvement by proper flat-fielding can be significant. There are three basic methods for flat-fielding, and their potential applications are described in turn:

Dome flats: They can be conveniently obtained at daytime. Their main use is the convenient inspection in the first afternoon of the cosmetic quality of the CCD's and to gain some practical operating experience with the instrument control system. In the B-band filter, the exposure time needed to achieve 60,000 electrons per (un-binned) pixel in is 2 seconds for a single bulb. For other passbands, scale this number according to the filter width (Sect. A.2) and the detector sensitivity (Sect. 2.5.1), keeping in mind that the colour temperature of the bulb is only about 3,000 K.

Only limited experience has been gathered with dome flat fields, and some improvement by placing the lamp at a better position or with a new reflective screen may still be accomplished. In the B-band filter, the ratio of a dome to a twilight flat shows a smooth peak-to-valley variation of 2.5%.

In contrast to other types of flat fields (see below), ESO does not maintain an on-line library of dome flats.

Twilight flats:

Since for these exposures the light path is the same as for the science exposures at night, twilight flats are useful for the correction of any residual large-scale inhomogeneities in the detector illumination. The somewhat higher colour temperature of the twilight also makes these data more comparable with the science exposures. They are therefore suitable for the correction of most multiplicative defects such as pixel-to-pixel sensitivity differences. By averaging a number of exposures with 20,000-50,000 ADU's, any detrimental effect of the photon and readout noise can be made negligible.

For wavelengths below 550 nm (TBC), where there is practically no fringing and the number and strength of night sky (air glow) lines are low, twilight flats are normally sufficient for adequate scientific results. But to observe in such a manner as to preserve the possibility to construct also "superflats" (see below), is in most cases still a good practice. Towards the long wavelength limit of the WFI "superflats" are necessary for the optimal cosmetic fidelity of images of extended objects.

For those filters, for which ESO maintains photometric calibrations (Sect. 4.3.3), the respective latest master twilight flats (i.e. the average of several individual exposures) are kept in the on-line calibration database (Sect. 6.3).

"Superflats": These are not the result of separate exposures but are extracted from the science exposures. For this purpose, all science exposures need to be scaled to the same level of background flux and put into a virtual 'vertical' stack. If the field is not too crowded and there are not too many extended sources, a given detector pixel in this stack will in most exposures only have seen the sky background so that a median filter can reject all the 'outliers' caused by sources falling on that pixel and retain only those pixels that have values around the mean background level. This can, for instance, be accomplished with MIDAS command AVERAGE/IMAGE.

If instead of one long exposure of a field several short ones are made with offsets that are small but larger than the typical size of the relevant objects ('dithering'), this procedure can also be very effective in eliminating particle events ('cosmic rays'). However, the cumulative effect of the readout noise needs to be kept in mind. Furthermore, the co-addition of multiple exposures must be done separately for each chip of the mosaic. Because of the small but finite misalignments between them (Sect. 2.5.1), even an offset, that is a pure translation in the pixel coordinate system of one chip, will be a translation plus a small rotation in the pixel coordinate system of another chip.

Such a superflat consists of two main components, namely scattered solar light, i.e. a continuum with absorption lines, and night sky emission lines. The former, if it could be isolated, could in principle be used in the same way as a twilight flat, albeit at a much poorer S/N. The latter are quasi-monochromatic and, therefore, lead to the occurrence of interference fringes within the CCD. Because these fringes do not modulate the signal detected from the sources observed, superflats are usually better subtracted from the science images. The result would then be divided by a twilight flat.

> Because the strength of night sky lines is very highly variable with time and their incidence on the chip may vary with telescope focus, etc., it is not generally possible to use off-the-shelf superflats. Those provided in TBD can, therefore, only serve as illustrations.

Note that the above is only a very condensed and simplified description of flat fielding issues. For advanced purposes, it is very advisable to study the relevant literature.

The Observing Template for flat fielding is described in Sect. 4.1.1.

Scattered light: TBD

4.3.3 Photometry

Sect. A.7 lists the fields with photometric standards which are included in the on-line database. A dedicated observing template (Sect. 4.1.1) makes their observations rather convenient. However, if you are using a number of filters, you should select the field yourself in order to ensure that the standards and the set of filters match each other as far as possible.

If you use broad-band filters and prefer to observe your own standards, make sure that the latter cover some range in colour so that the colour term in the transformation to the standard system is meaningful.

Mean extinction coefficients for a number of passbands can be extracted from the information provided under the La Silla WWW homepage (http://www.ls.eso.org/lasilla/atm_ext/extinction.html). Interpolation will give reasonable results for other wavelengths. However, for accurate results, nightly extinction coefficients need to be determined. This requires to observe the field with the photometric standards at a number of different airmasses, covering at least the range within which also the primary targets are observed.

4.3.4 Spectroscopy

The dispersion relation can be derived by using unresolved features in the spectra of Galactic field stars. It varies slightly across the FOV (TBC). The zeropoint needs to be inferred from the zeroth order. If, owing to crowding or usage of an unfavourable filter this is not possible, telluric lines may be useful in the red part of the spectrum. Otherwise, crude guesses can be obtained using possible filter cut-off edges or an astrometric transfer from a direct image.

4.3.5 Polarimetry

TBD

4.3.6 Astrometry

The on-line database (Sect. A.9) includes a number of astrometric standard fields. A pattern of multiple exposures that is suitable for the astrometric calibration of the CCD mosaic is implemented as a dedicated Observing Template (Sect. 4.1.1).

<u>Note</u> that even at high Galactic latitude there will always be a dozen or more stars with entries in one or more of the major astrometric catalogues in the field of view of the WFI. For many applications, this will be sufficient.

5 Observing

The observations are carried out from the air conditioned control room of the 2.2-m telescope which offers ample space for documents, etc. which the observer may need.

The user interacts with the instrument through DAISY+ (Sect. 5.3). The telescope is controlled by an operator who is present in the same room. Only for some observing sequences will the observer also have indirect, partial control over the telescope. For other procedural details see Sect. 3.

This section describes the various stages of the observing process and the tools that are available in support of it. A summarizing cookbook is offered in Sect. 5.19.

5.1 Safety

In case of an accute threat to the safety or integrity of people or equipment, the telescope operator has full authority to take all necessary decisions. The visitor may only request the 2.2-m Telescope Team Coordinator to override the operator's decision.

In order to protect the telescope optics against dust contamination, observations are not permitted into the wind at wind speeds between 14 and 20 m/s. Above 20 m/s, the dome has to be closed.

When the external relative humidity exceeds 90%, the dome needs to be closed because condensation would severely contaminate the main mirror. The dome may be re-opened after the humidity has stayed below 85% for at least 30 consecutive minutes.

5.2 Computers at the 2.2-m Telescope

5.2.1 The TCS Workstation (w2p2tcs)

This is an HP Apollo 735 machine exclusively dedicated to the Telescope Control System. It is off-limits for all other purposes.

5.2.2 The Instrument Control Workstation (w2p2ins)

This HP C-200 workstation with 512 Mbyte of RAM runs DAISY+ (Sects. 5.3 and 5.11) to control the instrument, acquire the data, and display the incoming new files on the Real Time Display (Sect. 5.13.1) on a second monitor. A 100 Gbyte RAID disk system is attached to it where all incoming new observations are stored by DAISY+.

Although off-line image processing is possible on this machine, users are for two main reasons strongly encouraged to do this only on the data reduction workstation (, `w2p2drs`, Sect. 5.2.3):

1. There is always the risk that computing activities interfere with the instrument control and data acquisition which may ultimately result in the irrecoverable loss of data.
2. Image processing will convert the files from the raw `INTEGER*2` format to `REAL*4`. Together with the intermediate files of all reduction steps, this will rapidly fill the high-data security RAID system. The latter is much more prudently used as an on-line data repository only. Only in this way is it possible to keep several nights worth of observation on-line for convenient trend analysis, comparison of different observations, etc. on the data reduction workstation.

   Note also that the file transfer rate is quite noticeably reduced when about 80% or more of the disk capacity is filled (the write head needs more time to reach a free disk segment).

5.2.3 The Data Reduction Workstation (w2p2drs)

In addition to the control computers, there is an HP J-2240 dual-processor workstation with 1 Gbyte of RAM, roughly 100 Gbytes of user disk space, and dual screen. A copy of any observation is delivered also to this workstation (Sect. 5.15). Apart from this there is no other logical or physical link between `w2p2ins` and `w2p2drs`. This ensures that work on this user workstation cannot in any way interfere with the data acquisition process.

The main purpose of this workstation is to support off-line data reduction and analysis by the observer. To this end, MIDAS, IRAF, and IDL are available.

A particularly useful tool on this workstation is `SkyCat` (cf. URL: http://archive.eso.org/skycat/skycat.html). It basically is the same product as the Real Time Display (RTD, Sect. 5.13.1) but in addition provides access to numerous catalogs of astronomical objects, incl. Hubble Space Telescope Guide Star Catalog, and the Digital Sky Survey. They are valuable for the quick identification of sources and the comparison with previous observations.

Observers may bring their own data and software provided it is embedded in one of MIDAS, IRAF, or IDL. Their installation is permitted on the data reduction workstation, w2p2drs, only. No assistance of any kind will be provided with the installation. **Any** unauthorized modification of the default system setup as offered by the Observatory is prohibited.

Peripheral devices compromise a monochrome laser printer, two Quantum 4000/7000 DLT drives for DLT IV cartridges, and a DAT drive.

5.2.4 Access to the Outside World

In order to minimize negative impacts on the real-time operations, the above three computers only have a minimum of software installations and, in particular, connections to the outside world. However, there is a separate X-terminal in the 2.2-m control room with direct access to the general-purpose computer system of the La Silla Observatory. Visitors can use from there the `guest` account the password of which is posted on the notice board outside the computer users room in the administration building. This account supports e-mail, `rlogin`, `telnet`, `netscape`, `ftp`, and all other standard computer utilities under the UNIX operating system (HP-UX).

5.3 Starting up DAISY+

DAISY+ is an enhanced, but completely re-structured derivative of the DAISY control software system already in use at the Dutch 90-cm and the Danish 1.5-m telescopes on La Silla. In the future, it may also be introduced at the ESO 1.5-m telescope.

After log-on as `daisy` (the password is posted in the control room), DAISY+ will be started automatically and the X Windows-based GUI will appear. In a separate `xterm`, which is also automatically opened, DAISY+ can be terminated and re-started by typing `stop_daisy` and `start_daisy`, respectively.

After re-start of DAISY+ remember to "attach" the camera via the "Real-time" pull-down menu of the RTD panel (Sect. 5.13.1). Otherwise, incoming images will not be automatically displayed on the RTD. Re-displaying images after they have been transmitted to the w2p2ins workstation is not currently possible.

5.4 Readying the Instrument

The instrument and the detector system are normally initialized by DAISY+ at the beginning of each session. In order to protect the extremely delicate glass of the WFI front lens against any hazard, there is a built-in protective shutter. It can be opened and closed with a switch on the instrument control electronics box. The latter is mounted on the outer side of the M1 cell, in its northeastern quadrant. You need to keep the switch pressed until the desired position indicator is lit (green: open; red: closed). When the switch is released, the red light will stay on whereas the green light will be switched off (as applicable).

Check that there are no obstacles the telescope could collide with when moving.

5.5 Starting up the Telescope

The Telescope Control System (TCS) is installed on an HP 735 workstation. Since the TCS is normally handled by the Telescope Operator, it is not described here.

5.6 Daily Health Checks

Every afternoon and after each night, a pair of bias exposures are taken, checked for pick-up noise patterns, and analysed to verify the readout noise level (in ADU's) of the CCD's.

Furthermore, the Observatory maintains a set of 12 fields with an approximate declination of –30 degrees and an average separation of 2 hours in right ascension.

Prior to the beginning of any scientific observations and at the end of every night, short exposures of the field closest to the meridian are made through the B and I filter. By comparison with archival reference observations kept on-line, this enables an automatic procedure running on the user workstation (Sect. 5.2.3) to quickly check (i) the pointing, (ii) the overall throughput of atmosphere, telescope, instrument, and detector, and (iii) the astrometric fidelity.

Note: Because these daily checks are vital for quality tracking, they are performed regardless of the actual scientific programme to be executed. The observations and their reduction are carried out by the telescope operator; the execution time is TBD minutes.

5.7 Focussing Telescope and Instrument

The camera does not have a focussing unit of its own, and focussing is accomplished by moving the secondary mirror of the telescope. A focus sequence can be invoked via the GUI of DAISY+ (Sect. 5.3). It consists of a number of exposures with different focal positions between which the charges on the CCD are shifted by a constant amount. The CCD is read out only at the end of the sequence. It is recommended to use at least 8 focus positions with a step size of 40-50 M2 encoder units and to shift the subimages by 50 CCD pixels. Even when some stars may be bright enough for very short exposures, do not use an exposure time of less than 15-20 seconds because only then is atmospheric image motion properly averaged out. Since the mosaic is fairly co-planar with the focal plane, only the CCD in position "a" of the mosaic (Fig. 4) is used in order to save time and disk space.

Although this may take a little bit of extra time, the periodic 240-second error in the telescope drive (Sect. 2.6.2) makes it advisable to use the autoguider also for the short exposures of a focus sequence.

The central focus position of the sequence can be chosen using the formula

$$\mathrm{focus(T)} = 25741 - 66 \times \mathrm{T}$$

where T is the temperature (in degrees centigrade) of the telescope serrurier. It is displayed and continually updated in the TCS control panel. The focus value is expressed in units of steps of the M2 encoder, one encoder step corresponding to 1.25 μm. The proportionality factor is negative because M2 has to move towards M1 in order to compensate a thermal expansion of the serrurier. Please note that there is an additional dependency of the focus on telescope position. Under good seeing conditions, a dedicated focus exposure may therefore still be a good investment.

A MIDAS procedure is available to fit a parabola to the variation of the FWHM of point sources with focus position in order to determine the best focus. Since also the peak flux values are displayed, it is possible to check that no subimage was saturated, i.e. reached a value of 65,535. When the autoguider has been used, the focus curves displayed for both x and y should coincide extremely well. Under reasonable observing conditions, the focus values returned for different stars in the same exposure should not scatter by more than 3-5 encoder units.

The depth of focus is about 50 M2 encoder units. Remember (Sect. 2.5.1.1) that the residual tilt of the CCD mosaic with respect to the focal plane amounts to less than 15 encoder units to which up to 20 encoder units need to be added for the position-dependent instrument flexure.

The focus needs to be checked (or adjusted according to the above formula) whenever the change in temperature since the last setting of the focus exceeds half a degree. Remember that *changes* of the PSF can also be checked by means of the autoguider (Sect. 5.12.1).

Because the filters are in the converging beam, they have some optical power. The offsets in focus with respect to the B filter are included in Tables 2 to 5; they are defined as follows:

$$\mathrm{focus}(X) = \mathrm{focus}(B) + \mathrm{offset}(X)$$

DAISY+ computes offsets w.r.t. to the set focus value assuming that the latter refers to the B filter. *It is, therefore, strongly recommended to take focus sequences only with this filter.* Otherwise it is necessary to calculate the focus for the B filter from the measured focus value and the offset for the filter used with the above formula.

5.8 On-line Creation of Observation Blocks*

TBD

5.9 Broker for Observation Blocks (2p2BOB)*

TBD

Loading OB's into DAISY+ includes an automatic check of the syntax and contents of the OB itself and the Observing Template signature files which it contains as described in Sect. 5.10.

5.10 Executing an Observation Block*

The execution of Observation Blocks is controlled via the "Observing" menu (TBD) of DAISY's GUI. Only one OB can be submitted for execution at a time. But several OB's can be marked in advance for sequential execution in any order. This can be changed at any time, and the observer may define the sequence of OB's to be executed automatically or only upon confirmation after each OB. The contents of OB's can be inspected and modified by TBD.

Before really executing an OB, DAISY+ repeats (Sect. 5.9) the following checks:

- Template names are recognized.
- All required parameters are provided.
- Parameters are of the correct type (integer, real, string).

- Numerical parameters are within their allowable ranges.
- Names of filters are recognized.
- There is only one target.
- The total exposure time must not be more than 95% of the remaining time after which the target will within 10 minutes reach the pointing limits of the telescope.

If one of these conditions is not fulfilled, DAISY+ stops and returns an error message. For unspecified parameters with default values, DAISY inserts them if required.

In the following cases, DAISY+ requests a confirmation by the user before proceeding:

- Detector setup parameters are different for different templates (only *within* an OB!).
- During (part of) the execution of an OB the airmass will exceed 2 (TBD).

After completion of an OB, DAISY+ issues an optical and acoustical signal. The same, but with different signals, happens if during the execution a problem occurs.

5.11 Defining and Executing Exposures within DAISY+

Exposures can also be defined and executed directly from the DAISY+ GUI. The latter is largely self-explanatory and not described here. Note the definition of 'single exposures': This can actually be a number of exposures (a repetition factor can be set; this can be useful for calibration exposures) which, however, use one and the same instrument set-up and exposure time.

If a number of exposures with different filters and/or exposure time is to be obtained, an 'exposure sequence' needs to be defined. Sequences can be saved in disk files for later re-usage.

For the monitoring of the progress of the observations, the status fields at the top of the DAISY GUI are very useful. They turn black (with labels in yellow) when a particular activity is on-going:

1. After an exposure has been requested, the `EXP. ACTIVE` field turns on.
2. When a filter has to be put into the beam, the `SETTING UP` field is activated.
3. The `INTEGRATING` field turns black when the actual exposure of the detectors has started. It remains on, i.e. black,until she shutter has been closed. A moving bar shows graphically which fraction of the exposure has elapsed.
4. That FIERA is busy reading out the image, is indicated by the `READING CCD` field. The rate of progress is visible as a colour bar keeps moving.
5. Finally, the fraction of the file transferred to the w2p2ins workstation is shown in the `TRANS. IMAGE` field. However, the same can be observed more instructively on the RTD (Sect. 5.13.1) where every file is displayed as it arrives on the workstation.
6. After completion of this full cycle, also the `EXP. ACTIVE` field goes off.

Note that only the instrument can be controlled by DAISY+. Pre- or off-setting the telescope, autoguiding, etc. are only possible from within the TCS GUI. The only exception is the stepping-through of the focus range during focus exposure sequences.

5.12 Keeping Track of the Observing Conditions

5.12.1 Monitoring Telescope Tracking and Variations of Sky Transparency and PSF with the Autoguider

The image of the guide star is displayed on the Real Time Display of the TCS at the actual frame rate. This already permits some crude visual impression of the prevailing atmospheric conditions and their stability.

Furthermore, the mean of the FWHM of the stellar image and its rms variation (both in arcsec) are computed and displayed for every readout of the tracker CCD. For a comparison with the data from the seeing monitor (Sect. 5.12.2) a graphical presentation with the data of the whole night can be requested as well. Note that the quantities are related only in so far as the FWHM is the convolution of the external seeing with the dome seeing, the telescope defocus, and the aberrations of the optics. Moreover, the FWHM of the image of the guide star is *not* equivalent to the average image quality over the FOV because it is already far off-center and the tracker CCD is not quite in the same plane as the mosaic. That is, the absolute numbers derived from the guide star require some critical evaluation. But their *variations* provide valuable diagnostics.

Something analogous is provided for the relative sky transparency (i.e., in arbitrary units). Similar statistical data for the corrections by the autoguider to the tracking of the telescope are presented as kind of a windrose diagram.

All these parameters are logged. An excerpt of the log files is part of the data products delivered to the applicants (Sect. 2.10).

5.12.2 The Meteorological Monitoring System

All relevant meteorological data external to the dome are updated every 2 minutes on the WWW (URL: http://www.ls.eso.org/lasilla/Telescopes/2p2T/meteo/meteomonitor.html#tab).

Current average values and graphical presentations for the past 24 hours are provided for air pressure, temperature, humidity, wind speed and direction, and seeing. The elevation angle of the Sun is also shown.

The seeing is determined by means of a dedicated small telescope ('DIMM' - Differential Image Motion Monitor) which measures the differential motions between two images of one star which is observed through two apertures. These motions have been carefully calibrated in terms of the image FWHM (in arcsec). Note that at the time of writing the operation of the seeing monitor had been suspended until further notice.

5.13 Checking an Observation

Although the Observatory tries hard to minimize faults by preventive maintenance and off-line quality control (Sect. 6.1), it is solely the responsibility of the observer to check the quality of the observations. This concerns especially but not only the scientific quality. Some means to do this are pointed out in this Section. If in doubt, the observer should contact the 2.2-m Telescope Team for advice.

5.13.1 On the Real Time Display

Upon read-out all images are sent to the Real Time Display attached to DAISY+ (Sect. 5.3) on workstation w2p2ins. The number of pre- and overscan pixels visible there approximately matches the physical width of the inter-CCD gaps in the mosaic. Therefore, the displayed images give a roughly representative impression of the projection of the detectors onto the sky.

The aim of the RTD is to enable the observer at the earliest possible moment to critically evaluate whether an observation fulfills the purposes it was made for. To this effect the data are transferred to the RTD at the same time as they come out of the CCD controller (FIERA, see Sect. 2.5).

In the case of the WFI, the BIG challenge is to provide this capability for images as large as some 70 million pixels. With today's most advanced display hardware technology, this many hardware pixels require an enormous number of devices, and, taking into account also the limited resolution of the human eye, a total screen size of at least $1\,\mathrm{m}^2$ would always be the minimum.

As a compromise, which still only offers a very limited solution, the VLT RTD (which in its display capabilities is largely identical to SkyCat [cf. URL: http://archive.eso.org/skycat/skycat.html]) follows a 3-stage approach:

- The full mosaic is displayed in a stamp-size format. This is accomplished by means of pixel skipping, i.e. without rebinning. Accordingly, only very coarse structures are visible because only of the order of 0.01% of the data is shown. For instance, the gaps between the chips are hardly detectable.
- In the above overview window, subwindows can be defined with the cursor and with various zoom factors displayed in the main window. This gives an overview of a portion of the file at full resolution.
- Another small window shows the area surrounding the cursor position in the main window. Here individual pixels can be inspected in full detail.

In both the overview and the main window, pixel values and coordinates can be read with the cursor. Auto-scaling of the dynamical range covered by the colour coding is available. In the main window numerous other functions are supported, e.g.: traces through the image, statistics, fitting of Gaussians to point sources, hardcopies, etc.

5.13.2 On the User Workstation

Two basic options exist: SkyCat (cf. URL: URL: http://archive.eso.org/skycat/skycat.html) and the image processing system of your choice (MIDAS, IRAF, IDL). For MIDAS, a special procedure which permits the data from the eight chips to be simultaneously loaded into displays on eight different work spaces is available on the HP terminal. They can be cycled through at a mouse click and of all display possibilities offer by far the best data-to-screen area ratio.

An exhaustive list of possible checks cannot be provided here. But the following should cover a wide range of situations:

A/D converter: Compute a histogram for a very flat portion of a low-exposure flat field. Make sure that the sampling step of the histogram is exactly 1 ADU. Check that there is no periodic pattern in the histogram.

Bias variations: Compare values of pre- and overscan pixels of exposures taken at different times. Or compare bias frames taken at different times.

CCD pickup noise: Display un-binned flat field or sky exposure *without zoom-down*, i.e. at most one image pixel per display pixel. Use full range in brightness and color for a narrow range around the mean background level. Look for any non-random pattern.

CCD saturation: Check that the flux does not reach 65,535 ADU's in any pixel (only exception: particle events and hot pixels/columns).

Focus uniformity: Fit Gaussians to point sources over the entire FOV. Compare the FWHM's. This is most conveniently done with the "pick object" function of the RTD.

Scattered light: Display an image such that the entire dynamical range in brightness and colour of the display is used for a narrow range in exposure level from slightly below to slightly above the mean background level. Check for large-scale structures that do not repeat on exposures of other fields. However, beware of variations of the sky background with level of airglow activity and solar elevation angle.

Straylight: Compare flat field exposures with reference flat field in on-line database (Sect. 6.3). (If still possible, check that all lights are off in the dome.)

Throughput: Compare your results with those of the exposure time calculator (make sure that the parameters are the same).

Other: TBD

5.14 Checking out the Detector

A couple of simple points are listed in Sect. 5.13.2. For deeper checks, there are several dedicated MIDAS procedures (TBD) and the `CCD` context in MIDAS.

5.15 Data Handling

The on-line data flow consists of the following steps (all timings refer to an insignificant additional load on the machine):

- At the end of an exposure, FIERA (Sect. 2.5) reads out the CCD's. This takes 27 seconds.
- In parallel and at the same rate, FIERA sends the data to the Real Time Display (Sect. 5.13.1) attached to DAISY+ (Sect. 5.3).
- Also in parallel, FIERA transmits the data to the instrument workstation, w2p2ins (Sect. 5.2), and DAISY+ which writes them to disk (in FITS format, Sect. A.10.1). The re-formatting and writing to disk is slower than the readout and in addition to the 27 seconds readout time requires additional $\leq$10 seconds.
- After its full arrival on w2p2ins, DAISY+ copies the FITS file within 45 seconds to the data reduction workstation, w2p2drs.
- Once on disk, the FITS files are on w2p2ins and w2p2drs are copied to two separate DLT drives as a safe backup. This takes about 210 seconds for a full frame.
- An automatic background process converts the FITS file on the disk of w2p2drs to the format used by the off-line data reduction system (MIDAS, IDL, or IRAF) selected by the user.

In FITS format, one complete raw frame takes about 142 Mbytes so that about 500 of them can be stored on one 70-Gbyte DLT (using hardware compression by the DLT drive). But after any operation on disk that converts the data into floating point format, the size of a full frame will be 285 Mbyte. The disk space available on the user workstation is roughly 100 Gbytes; accordingly, users have to manage the database with some prudence.

A new DLT is mounted at the beginning of every observing session. It is replaced with a new one if it is full. All tapes are sent to the VLT Science Archive (Sect. 7) at ESO Headquarters in Garching. The second tape is given to the user.

At daytime, users may copy files to DLT when the drives are not in use for the routine data saving. A DDS3 DAT drive is available at any time but a 125m DDS3 (12-Gbyte) tape can only accommodate ~88 raw files. With (hardware) compression, the capacity increases by about a factor of 1.5. A DDS3 can handle DDS2 tapes (without compression, the capacity of a 120m DDS2 tape is 4 Gbyte) whereas a DDS2 drive cannot read DDS3 tapes. Accordingly, before using DDS3 tapes, visitors should make sure that these tapes can be read at their home institutes.

Note that ESO reserves the right to charge Visiting Astronomers for data storage media they wish to take with them to their home institutes.

5.16 Operations Support Reports

At the end of the night, operator and observer prepare and submit the obligatory daily night report and, if something needs attention by day-time support staff, the problem report. This is done by filling in the forms accessible on the Web (URL: http://www.ls.eso.org/lasilla/Reports/html/Opreport.html).

Forms for the submission of instrument setup and other requests as well general comments can be activated from the same WWW page.

Note that both problem reports and setup requests need to reach the 2p2 Team one hour before sunrise at the latest.

Via the same WWW page the existing databases composed of these reports and requests can also be queried, and their status can be checked. In this way observers can find out already in advance whether there are any not-yet-solved problems that could affect their observations.

Any interventions by day-time support staff and their results/effects are communicated to the observer by TBD.

At the end of an observing run, an end-of-mission report is required. The corresponding form is available on the Web page mentioned above.

5.17 Utilities

In the control room, the following useful items are available to the observer:

- a copy of this user manual
- user guides for MIDAS, IDL, and IRAF
- a copy of the relevant edition of the Astronomical Almanac and its Explanatory Supplement
- catalogs: TBD

5.18 Shutdown Steps

Normally, the telescope operator will

- close the M1 cover of the mirror,
- move the telescope to the zenith,
- close the dome slit,
- turn the dome to its parking position,
- refill the dewar,
- enter dewar pressure and CCD temperature in the log sheet on the southern wall of the dome,
- shut down the TCS,

– switch off all lights.

It is the duty of the observer to

– close the protective shutter of the WFI (Sect. 5.4),

– ensure that all data have been properly saved to tape,

– terminate DAISY+,

– write the Operations Support Report (Sect. 5.16).

5.19 Cookbook

(This section is not meant to be a quick by-pass of the main body of the manual for those who are always short of time.)

Before the night starts:

- Agree with the telescope operator on the time, when the dome should be opened.
- Check that the dewar was filled (the log sheets are on the southern wall of the dome). The temperature should be 169±0.2 K and the pressure below 2×10^{-5} mbar.
- Mount a DLT in the drives attached to `w2p2ins` and `w2p2drs`.
- Start up DAISY+. Remember to attach the camera to the RTD.
- Take a couple of bias exposures to clean out the detector system.
- Compute the difference between two bias exposures. Calculate the rms in a region free of detector blemishes, divide by $\sqrt{2}$, and compare with the read noise (in ADU's) given in Sect. 2.5.1.1.
- Compare the coordinates of the Moon with those of your objects.
- Check the satellite images on ESO's meteorology Web page (URL: http://www.hq.eso.org/observing/weather/).
- Open the protective shutter of the WFI.
- Take twilight flat field exposures as required by your project. (It has been noticed that at certain combinations of time and telescope position angle light reflected off the aluminium panels of the Schmidt telescope building can have disturbing effects.) Make sure, that telescope and dome slit are pointing away from the sun!

During the night:

- If you need photometric standards, observe them first, because they do not require a perfectly dark sky or a good focus. Too early a focus sequence can often be waste of time because the temperature of the telescope serrurier will usually continue to drop for a while.
- Observe the daily health check fields at the beginning and the end of the night.
- Regularly check the sky for clouds. Especially in the summer, monitor the external humidity provided on the Web (URL: http://epu.ls.eso.org/lasilla/dimm/meteo/) by the La Silla MeteoMonitor Station. On the same page, the wind speed and direction are logged. High-velocity wind is mainly a concern in the winter.
- With DAISY+ monitor the amount of free disk space on w2p2ins. Use UNIX command `bdf` on w2p2drs.
- If photometric calibrations are needed, observe standard star fields approximately every 2 hours and at different airmass.
- For each exposure:

- Ask the telescope operator to preset the telescope to your field and to acquire a guide star.
- Select filter, CCD binning pattern, and exposure type and time with DAISY+.
- Check telescope focus against temperature of telescope serrurier (available on TCS main control panel). If you change the telescope position by a major amount, consider taking a new focus sequence.
- Start exposure (when autoguider is ready)
- Fill in log sheet with details of exposure.
- Regularly monitor DAISY+ control panel for error messages and exposure status.
- Monitor temperature variations of serrurier.
- Move dome, telescope, and filter for next exposure only after CCD readout is complete (DAISY+ control panel) to avoid possible pick-up noise (remaining pure file transfer phase is not critical).
- After the exposure, use the RTD to check image quality (incl. homogeneity across field), background level, etc.
- If you need to close the gaps between the chips, remember that in order to have at least 3 data points everywhere (this is the minimum for median filtering of the stack of images), observations at 5 different positions have to be taken. When choosing the offset values, bear in mind that in right ascension the relatively unvignetted field of view of the tracker is CCD is only about 200 arcsec wide. In declination the full range of about 1000 arcsec can be exploited. If possible, the guide star should be selected such that the offsets do not move it beyond the useful field of the tracker CCD. Otherwise, combined offsets would become impossible, and a new guide star acquisition exposure had to be taken.

After the night:

- Take more twilight flats.
- Close the protective shutter of the instrument.
- Together with the telescope operator, check temperature and pressure of dewar.
- Save all data.
- Fill in the Operations Support Report.
- Exit from DAISY+.

6 Data Reduction and Calibration*

It is ESO's aim that the WFI delivers data of quantitatively well-understood quality. Continuous quality control (Sect. 6.1) forms the core of this effort. Quantitative quality control necessarily implies quantitative calibrations (Sect. 2.9). However, not every instrument mode or option needs to be calibrated in order to gain confidence that telescope and instrument are performing nominally. In order to understand what is actually done, it is therefore necessary to read Sect. 2.9 carefully.

For those instrument modes that are regularly checked and calibrated, ESO applies the established standard calibration relations in a pipeline procedure (Sect. 6.2) and delivers the results to the applicants (Sect. 2.10). The results *do not pretend* to be the best ones possible and may also not always have the cosmetic quality that is desirable for publications (for instance, particle events are only in some cases removed).

6.1 Quality Control*

Except for calibration exposures, the scope of automatic quality control is necessarily limited to very basic points. Only very few files can be inspected by ESO staff at the level of detail proposed in Sect. 5.13.2. It is the responsibility of the user of the data to verify their qualification for the intended purposes.

6.1.1 Science Frames*

Quality control of the science exposures is part of the pipeline processing (Sect. 6.2). It is done on all science frames regardless of whether they will also be processed any further.

It is very important to note that the scientific *usefulness* or value of the frames *cannot* be checked (limiting magnitude, actual image size, background level, signal-to-noise ratio, etc.).

Checks that will be done include the following:

Dynamical range: If the dynamical range is zero (maximum $\equiv$ minimum), the frame will be flagged to be invalid since the information content is zero.

Comparison with user requirements: For the following parameters a comparison between the actual observing conditions and the user-supplied requirements will be performed:

- seeing (as measured by the external seeing monitor - Sect. 5.12.2)
- sky transparency (as signalled by the seeing monitor and the autoguider - Sects. 5.12.1 and 5.12.2)
- date and time (if time-critical observations)
- phase of the Moon
- field coordinates

Calibration data: It is checked whether calibration data suitable for standard pipeline processing (if foreseen) are available.

6.1.2 Calibration Exposures*

Quality checks on calibration frames depend on the type of exposure:

Bias:

- mean level
- variance

Flat field:

- filter
- source
- exposure time
- mean exposure level
- homogeneity of illumination

Photometric standards:

- filter
- field coordinates
- airmass
- background level
- PSF size (comparison with seeing monitor and autoguider)
- overall sensitivity

Astrometric standards:

- filter
- field coordinates
- airmass
- centering of field
- PSF size (comparison with seeing monitor and autoguider)
- rms of plate solution

6.2 The Pipeline*

Data obtained in all modes, for which the Observatory continually maintains a calibration, will be automatically processed by a so-called pipeline. The data will be processed twice:

On-line: For the on-line run, only the latest calibrations derived from previous calibration observations are used. They are taken from the on-line Calibration Database (Sect. 6.3). Even if suitable calibration data are obtained within the same night, they will not be used for the on-line reduction. The results of the on-line pipeline reduction will not be saved. The on-line pipeline may also be simpler than the off-line version.

Off-line: During the off-line run, those calibrations will be used that experience has shown to probably be the most suitable for the purposes of the pipeline (Sect. 6.2.1). The pipeline does not distinguish between data obtained in service or visitor mode. If during the course of an observing programme dedicated calibration observations were made, they may or may not be used by the pipeline even if they are compatible with the requirements of the pipeline. The FITS header of the pipeline-processed data (Sect. A.10.2) fully documents which calibration data have been used (see also Sect. 2.10).

6.2.1 Scope*

The purpose of the pipeline is to calibrate the data to the extent and level specified in Sect. 2.9. It is *not* a solution to everything. Users may not find it difficult to achieve a more accurate calibration by using the same calibration data but a more sophisticated procedure than a mass production engine such as the pipeline can afford. They will also notice that a better cosmetic quality (e.g., fringing, particle events) can often be desirable.

6.2.2 Quality Control*

TBD

6.2.3 Photometry*

TBD

6.2.4 Spectroscopy*

The processing only consists of bias subtraction and division by a flat field.

6.2.5 Polarimetry*

TBD

6.2.6 Astrometry*

TBD

6.3 The Calibration Database*

TBD

6.3.1 Astronomical Data*

TBD

6.3.2 Instrument Data*

TBD

6.4 Off-line Data Reduction

Apart from the calibrations applied to some data by the pipeline (Sects. 2.9 and 6.2), off-line data processing is the responsibility of the applicants. ESO does not currently offer any WFI-specific data reduction tools. But the following subsections aim at providing some advice on general strategies. One of the most basic rules is to reduce calibration and science data as much as possible in the same way. A simple self-consistency check is to apply all calibration steps to the raw calibration data and to compare the results with the expectation. For instance, if the magnitudes of photometric standard stars after the reduction come out completely different from the tabulated values, something has obviously gone wrong. (Clearly, these two rules are only necessary but not sufficient to ensure optimal results.)

Some hints for quality checks are given in Sect. 5.13.2.

6.4.1 Bias Correction

The bias is an electronically added baseline signal which during the reduction needs to be subtracted from the exposures. To this end, it is sufficient to determine the mean signal in a couple of frames. Since, owing to the nature of the bias signal, it is supposed to be the same for all pixels (and only changed by the addition of the readout noise – but see below for a more differentiated description), only that number should need to be subtracted. Subtracting a frame or only the average of several frames would only add unnecessary noise.

If bias exposures have been taken throughout the observing run, they can be used to check on the constancy of the performance of the detectors (Sect. 5.14).

Remember that the pre- and overscan pixels present for each CCD (Sect. 2.5.1) also contain the bias signal. Moreover, this information can be used to check whether the presence of a strong exposure in a given region of the CCD has affected the local bias level. This effect can, for instance, be studied by comparing flat field exposures of very different exposure levels. Although the difference is only very few ADU's, it can become an important source of *apparent* non-linearity in low-light level exposures.

6.4.2 Flat Field Correction

Sect. 4.3.2 discusses at length which basic strategies are most promising and for what reasons. The best results are often obtained by using a combination of twilight and "super flat fields". Both need to be bias-subtracted. For frames with significant exposure level, the bias value deduced from the pre- and overscan pixels often yields better results than using a dedicated bias exposure (Sect. 6.4.1). Thereafter, one would subtract the "super flat field" from the bias-corrected science exposure and divide the result by the twilight flat. Trial-and-error methods can often give further insights, especially in the case of problems that result from stray- or scattered light.

6.4.3 Photometry

TBD

6.4.4 Spectroscopy

TBD

6.4.5 Polarimetry

TBD

6.4.6 Astrometry

TBD

7 The Archive

All raw WFI frames obtained by ESO observers are also copied to the ESO Science Archive. After a proprietary period of one year they will become publically available.

A Appendices

A.1 Cosmetically Deficient CCD Columns

Table 7: Hot columns of the CCD's in the top group of the mosaic. Row numbers denote where the defect starts (cf. Sect. 2.5.1.2); the "≤" and "≥" signs give the direction of the defect (*all* subsequent pixels in the given column are affected). Column and row numbers are counted starting with the first southeastern ligh-sensitive pixel of each CCD. The numbers have been compiled carefully but can only be regarded as indicative. 8)

Chip #50		Chip #51		Chip #52		Chip #53	
Col. No.	Row No.	Col. No.	Row No.	Col. No.	Row No.	Col. No.	Row No.
570	≤2900	78	≤2007	1088	≤1214	80	≤1575
659	≤3402	137	≤2044	1339	≤2717	104	≤1600
1013	≤3036			1890	≤2345	269	≤1570
1014	≤3036			1956	≤2091	340	≤1
1083	≤3149			1987	≤1295	341	≤1
1084	≤3049			2013	≤2116	342	≤1
						372	≤1785
						374	≤1760
						593	≤3060
						631	≤1
						644	≤3060
						677	≤1
						683	≤1
						688	≤2617
						719	≤860
						720	≤1622
						726	≤2520
						731	≤1892
						750	≤1
						840	≤1725
						849	≤1337
						856	≤1430
						880	≤2361
						891	≤2147
						903	≤1555
						940	≤1922
						956	≤2131
						970	≤814
						1138	≤1223
						1715	≤1190

Table 8: Same as Table 7 except for bottom row of CCD's

Chip #57		Chip #56		Chip #55		Chip #54	
Col. No.	Row No.	Col. No.	Row No.	Col. No.	Row No.	Col. No.	Row No.
12	$\geq$2047	2	$\geq$1	50	$\geq$1056	1198	$\geq$927
76	$\geq$914	15	$\geq$1571	251	$\geq$1672	1259	$\geq$358
77	$\geq$914	19	$\geq$2124	335	$\geq$1		
144	$\geq$333	29	$\geq$1	507	$\geq$225		
154	$\geq$1693	46	$\geq$2255	765	$\geq$362		
219	$\geq$1756	65	$\geq$1706	903	$\geq$1		
288	$\geq$1762	75	$\geq$1461	1048	$\geq$229		
300	$\geq$510	131	$\geq$2036	1628	$\geq$994		
304	$\geq$1848	135	$\geq$1468	1766	$\geq$337		
469	$\geq$556	144	$\geq$1034				
1171	$\geq$1	146	$\geq$1571				
1495	$\geq$3312	193	$\geq$1				
		231	$\geq$2384				
		252	$\geq$2416				
		267	$\geq$1310				
		307	$\geq$15				
		320	$\geq$1				
		336	$\geq$1477				
		433	$\geq$1165				
		1316	$\geq$1561				

Table 9: Same as Tables 7 and 8 except for dark columns

Chip #50		Chip #51		Chip #52		Chip #53	
Col. No.	Row No.	Col. No.	Row No.	Col. No.	Row No.	Col. No.	Row No.
1147	$\leq$1						
1148	$\leq$1						
1149	$\leq$1						
1150	$\leq$1						
1151	$\leq$1						
1152	$\leq$1						
1153	$\leq$1						
1154	$\leq$1						
1155	$\leq$1						
1156	$\leq$1						
Chip #57		Chip #56		Chip #55		Chip #54	
Col. No.	Row No.	Col. No.	Row No.	Col. No.	Row No.	Col. No.	Row No.
707	$\geq$2435	682	$\geq$1899	1261	$\geq$479	257	$\geq$862
708	$\geq$2435	948	$\geq$1848			1068	$\geq$3772
1663	$\geq$3084	1931	$\geq$2962			1069	$\geq$3772
						1553	$\geq$ 807
						1690	$\geq$3346
						1691	$\geq$3346

A.2 Filter Transmission Curves

This section is subdivided by the bandwidth of the filters (broad, medium, and narrow) and within each subsection sorted by central wavelength. All transmission curves are measured at the center of the filter. **Note** that the most up-to-date and complete information is *only* available on the WWW page mentioned in Sect. 1.1.

A.2.1 Broad-band Filters

TBC

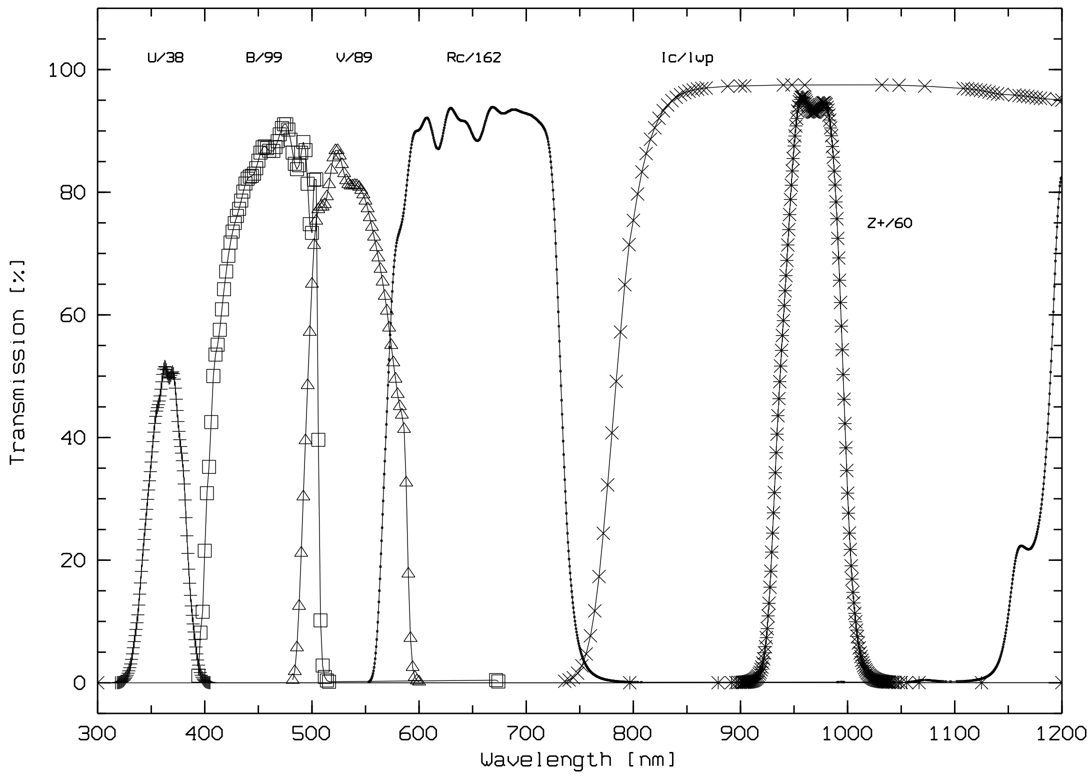

Figure 11: Transmission curves for the broad-band filters as labeled

A.2.2 Medium-band Filters

TBC

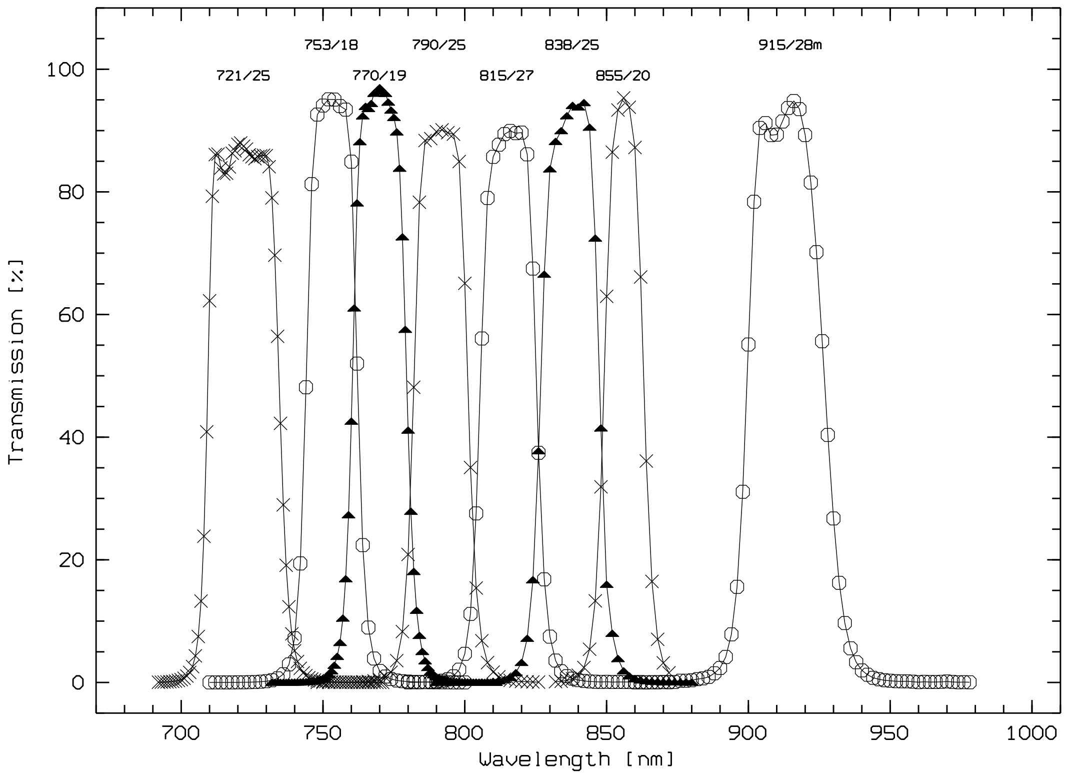

Figure 12: Transmission curves for red medium-band filters as labeled

A.2.3 Narrow-band Filters

TBC

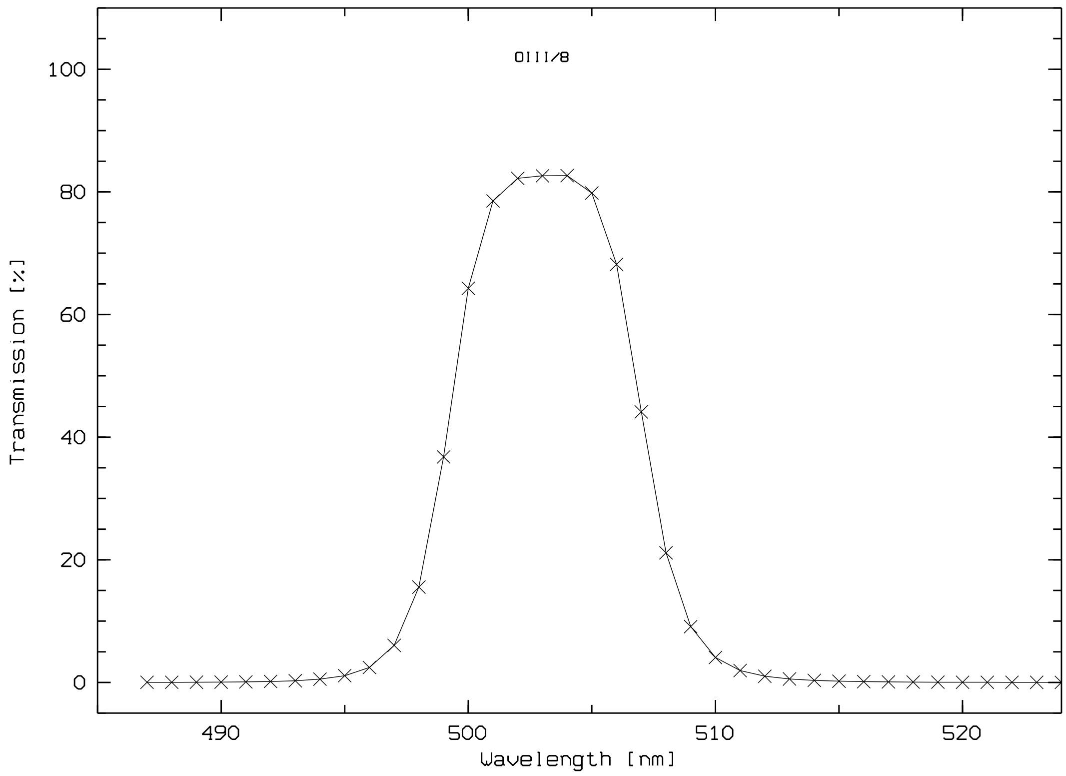

Figure 13: Transmission curves for visual narrow-band filters as labeled

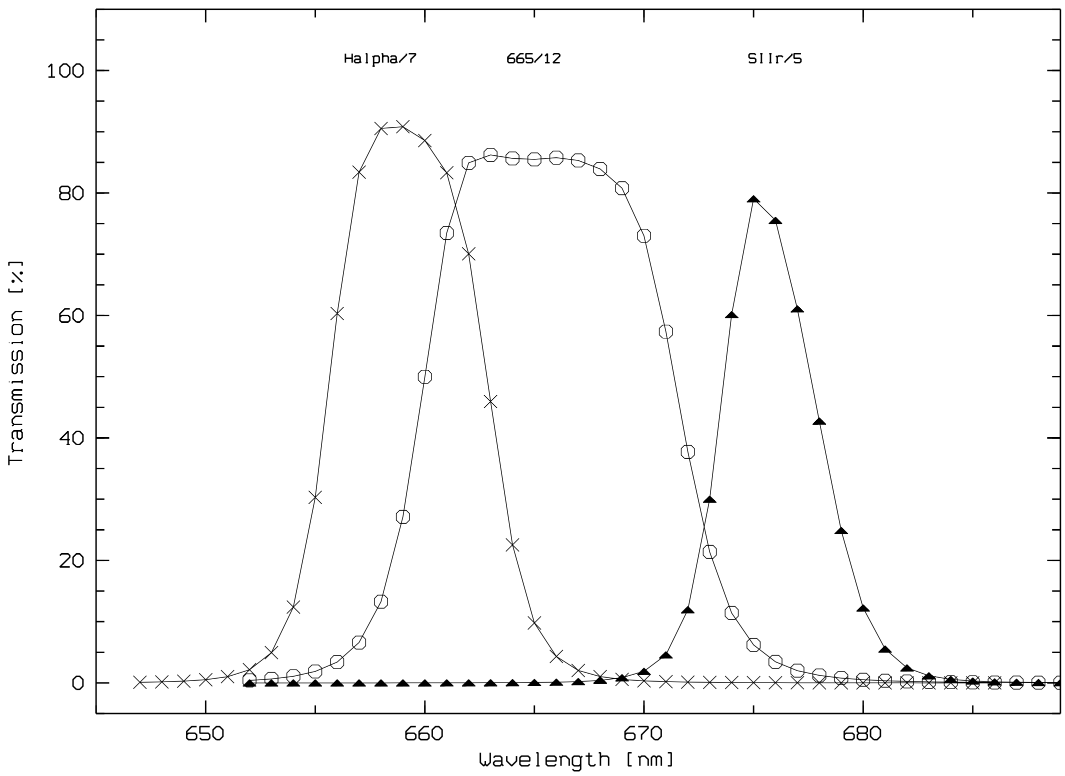

Figure 14: Transmission curves for red narrow-band filters as labeled

A.3 Filter Transmission Tables

This section is subdivided by the bandwidth of the filters (broad, medium, and narrow) and within each subsection sorted by central wavelength. The transmission data refer to the center of the filter. Values below 0.1% are omitted.

A.3.1 Broad-band Filters

Table 10: Transmission data for filter B/99 (ESO # 842)

Wavelength nm	Transmission %	Wavelength nm	Transmission %	Wavelength nm	Transmission %
312	0.1	340	36.0	368	37.9
314	0.3	342	40.0	370	34.6
316	0.8	344	43.2	372	28.7
318	1.4	346	45.0	374	21.6
320	2.5	348	46.4	376	15.8
322	4.2	350	49.1	378	11.6
324	6.5	352	51.4	380	8.3
326	8.9	354	51.2	382	5.4
328	12.0	356	49.9	384	3.0
330	16.3	358	50.0	386	1.6
332	20.7	360	50.7	388	0.7
334	24.7	362	49.0	390	0.3
336	28.6	364	44.8	392	0.1
338	32.3	366	40.7		

Table 11: Transmission data for filter B/99 (ESO # 842)

Wavelength nm	Transmission %	Wavelength nm	Transmission %	Wavelength nm	Transmission %
394	1.2	436	80.1	480	88.6
396	8.2	438	81.4	482	86.5
398	11.6	440	82.2	484	84.6
400	21.5	442	82.5	486	83.7
402	30.9	444	82.7	488	84.4
404	35.2	446	83.0	490	86.4
406	42.5	448	83.9	492	88.2
408	50.0	450	85.1	494	86.9
410	53.5	452	86.5	496	81.4
412	55.1	454	87.3	498	74.8
414	57.6	456	87.5	500	73.4
416	60.9	458	87.2	502	82.0
418	64.2	460	86.8	504	82.1
420	67.1	464	86.7	506	39.6
422	69.6	466	87.4	508	10.2
424	71.8	468	88.3	510	2.8
426	73.6	470	89.4	512	0.9
428	75.0	472	90.5	514	0.4
430	76.1	474	91.1	516	0.2
432	77.3	476	91.1	672	0.4
434	78.6	478	90.2	674	0.2

Table 12: Transmission data for filter V/89 (ESO # 843)

Wavelength nm	Transmission %	Wavelength nm	Transmission %	Wavelength nm	Transmission %
482	0.4	522	86.8	562	69.3
484	1.9	524	86.8	564	67.5
486	5.7	526	85.9	566	65.4
488	12.5	528	84.5	568	63.1
490	21.2	530	83.1	570	60.7
492	30.4	532	81.9	572	57.9
494	39.5	534	81.3	574	55.1
496	48.5	536	81.1	576	52.2
498	57.2	538	81.1	578	49.5
500	65.0	540	81.2	580	47.1
502	71.4	542	81.1	582	45.1
504	75.3	544	80.9	584	43.7
506	77.2	546	80.3	586	41.4
508	77.6	548	79.6	588	32.6
510	77.6	550	78.6	590	17.8
512	78.0	552	77.3	592	7.3
514	79.3	554	75.9	594	2.5
516	81.3	556	74.3	596	0.9
518	83.6	558	72.7	598	0.4
520	85.7	560	71.0	600	0.2

Table 13: Transmission data for filter Rc/162 (ESO # 844)

Wavelength nm	Transmission %	Wavelength nm	Transmission %	Wavelength nm	Transmission %
556	0.9	676	92.9	1060	0.2
560	5.9	680	92.9	1064	0.3
564	18.9	684	93.2	1068	0.4
568	36.1	688	93.4	1080	0.3
572	52.7	692	93.3	1084	0.3
576	66.6	696	93.1	1096	0.2
580	72.6	700	92.8	1104	0.2
584	75.1	704	92.6	1112	0.3
588	80.3	708	92.1	1120	0.5
592	86.5	712	91.4	1124	0.6
596	89.7	716	90.6	1128	0.8
600	90.2	720	88.7	1132	1.2
604	91.4	724	82.9	1136	1.9
608	92.1	728	69.5	1140	3.0
612	90.0	732	50.8	1144	5.1
616	87.4	736	33.1	1148	8.7
620	87.8	740	20.2	1152	14.0
624	91.0	744	12.2	1156	19.4
628	93.5	748	7.3	1160	22.1
632	93.3	752	4.4	1164	22.2
636	92.1	756	2.8	1168	21.8
640	91.7	760	1.8	1172	22.1
644	91.4	764	1.2	1176	23.9
648	90.2	768	0.9	1180	27.7
652	88.7	772	0.6	1184	34.5
656	88.6	776	0.4	1188	45.4
660	90.3	780	0.3	1192	60.5
664	92.7	792	0.2	1196	76.1
668	93.9	804	0.1	1200	82.5
672	93.6	1056	0.1		

Table 14: Transmission data for filter Ic/lwp (ESO # 845)

Wavelength nm	Transmission %	Wavelength nm	Transmission %	Wavelength nm	Transmission %
736	0.2	820	90.5	1072	97.3
740	0.5	824	92.1	1108	96.9
744	0.8	828	93.3	1112	96.9
748	1.5	832	94.2	1116	96.8
752	2.8	836	94.9	1120	96.7
756	4.7	840	95.5	1124	96.6
760	7.7	844	95.9	1128	96.5
764	11.7	848	96.2	1132	96.3
768	17.3	852	96.5	1136	96.2
772	24.4	856	96.7	1140	96.0
776	32.3	860	96.8	1144	96.0
780	40.7	864	96.9	1156	95.8
784	49.2	868	97.0	1160	95.8
788	57.2	888	97.3	1164	95.7
792	64.9	900	97.3	1168	95.6
796	71.4	904	97.3	1172	95.5
800	75.4	940	97.5	1176	95.4
804	79.7	948	97.5	1180	95.3
808	83.3	960	97.5	1184	95.2
812	86.3	1032	97.5	1196	95.1
816	88.7	1048	97.4	1200	95.0

Table 15: Transmission data for filter Z+/60 (ESO # 846)

Wavelength nm	Transmission %	Wavelength nm	Transmission %	Wavelength nm	Transmission %
900	0.1	951	89.5	1002	23.3
903	0.1	954	93.9	1005	14.7
906	0.1	957	95.5	1008	9.1
909	0.2	960	95.2	1011	5.5
912	0.4	963	94.1	1014	3.3
915	0.8	966	93.3	1017	2.0
918	1.6	969	93.1	1020	1.3
921	3.4	972	93.5	1023	0.8
924	7.1	975	94.2	1026	0.5
927	14.0	978	94.6	1029	0.4
930	24.4	981	93.8	1032	0.2
933	36.2	984	90.8	1035	0.2
936	46.9	987	84.8	1038	0.1
939	56.2	990	75.7	1041	0.1
942	64.9	993	63.5	1044	0.1
945	73.9	996	49.5	1047	0.1
948	82.6	999	35.4		

A.3.2 Medium-band Filters

TBC

Table 16: Transmission data for filter 721/25 (ESO # 847)

Wavelength nm	Transmission %	Wavelength nm	Transmission %	Wavelength nm	Transmission %
696	0.12	715	82.93	734	56.44
697	0.17	716	83.04	735	42.25
698	0.22	717	84.07	736	28.96
699	0.33	718	86.30	737	19.10
700	0.46	719	86.70	738	12.35
701	0.68	720	87.75	739	7.92
702	1.04	721	87.99	740	5.16
703	1.63	722	87.45	741	3.41
704	2.58	723	86.99	742	2.29
705	4.33	724	86.04	743	1.56
706	7.49	725	85.74	744	1.09
707	13.26	726	85.42	745	0.76
708	23.85	727	85.75	746	0.57
709	40.87	728	85.86	747	0.40
710	62.24	729	85.97	748	0.30
711	79.29	730	85.91	749	0.23
712	86.08	731	84.10	750	0.18
713	86.16	732	79.02	751	0.13
714	83.91	733	69.67	752	0.10

Table 17: Transmission data for filter 753/18 (ESO # 848)

Wavelength nm	Transmission %	Wavelength nm	Transmission %	Wavelength nm	Transmission %
728	0.12	746	81.26	764	22.40
730	0.20	748	92.60	766	8.95
732	0.36	750	94.08	768	3.91
734	0.67	752	95.09	770	1.87
736	1.34	754	95.06	772	0.97
738	2.94	756	94.00	774	0.55
740	7.22	758	93.41	776	0.33
742	19.41	760	84.92	778	0.20
744	48.14	762	52.00	780	0.14

Table 18: Transmission data for filter 770/19 (ESO # 849)

Wavelength nm	Transmission %	Wavelength nm	Transmission %	Wavelength nm	Transmission %
743	0.10	763	88.19	783	11.77
744	0.13	764	92.40	784	7.67
745	0.17	765	93.96	785	5.05
746	0.23	766	93.61	786	3.53
747	0.28	767	94.42	787	2.44
748	0.36	768	96.09	788	1.78
749	0.49	769	96.53	789	1.27
750	0.68	770	97.00	790	0.94
751	0.93	771	96.43	791	0.73
752	1.32	772	96.06	792	0.57
753	1.90	773	94.64	793	0.45
754	2.81	774	93.34	794	0.36
755	4.26	775	92.16	795	0.29
756	6.52	776	89.78	796	0.22
757	10.50	777	83.86	797	0.18
758	16.92	778	72.67	798	0.15
759	27.35	779	57.59	799	0.11
760	42.61	780	41.15	800	0.10
761	61.08	781	27.92		
762	78.21	782	18.11		

Table 19: Transmission data for filter 790/25 (ESO # 850)

Wavelength nm	Transmission %	Wavelength nm	Transmission %	Wavelength nm	Transmission %
764	0.10	784	78.31	804	15.41
766	0.17	786	88.37	806	6.80
768	0.27	788	88.69	808	3.23
770	0.46	790	89.83	810	1.69
772	0.85	792	90.11	812	0.93
774	1.68	794	89.65	814	0.55
776	3.55	796	89.41	816	0.34
778	8.29	798	84.94	818	0.22
780	20.86	800	65.08	820	0.15
782	48.13	802	35.06	822	0.10

Table 20: Transmission data for filter 815/27 (ESO # 851)

Wavelength nm	Transmission %	Wavelength nm	Transmission %	Wavelength nm	Transmission %
788	0.10	810	85.71	832	3.57
790	0.16	812	87.69	834	1.83
792	0.28	814	89.41	836	1.02
794	0.52	816	89.94	838	0.61
796	1.01	818	89.57	840	0.38
798	2.09	820	89.66	842	0.24
800	4.67	822	86.12	844	0.16
802	11.17	824	67.49	846	0.11
804	27.57	826	37.45	848	0.08
806	56.09	828	16.82	850	0.11
808	79.01	830	7.46		

Table 21: Transmission data for filter 838/25 (ESO # 852)

Wavelength nm	Transmission %	Wavelength nm	Transmission %	Wavelength nm	Transmission %
808	0.11	832	88.24	856	1.90
810	0.18	834	89.99	858	1.08
812	0.28	836	92.42	860	0.63
814	0.49	838	94.11	862	0.41
816	0.85	840	93.85	864	0.30
818	1.59	842	94.57	866	0.21
820	3.26	844	90.56	868	0.15
822	7.21	846	72.47	870	0.10
824	16.75	848	41.51	872	0.12
826	37.78	850	16.01	874	0.10
828	66.58	852	8.02		
830	83.76	854	3.90		

Table 22: Transmission data for filter 855/20 (ESO # 853)

Wavelength nm	Transmission %	Wavelength nm	Transmission %	Wavelength nm	Transmission %
840	1.2	852	86.5	864	36.1
842	2.4	854	93.3	866	16.5
844	5.4	856	95.3	868	7.0
846	13.3	858	93.8	870	3.2
848	31.9	860	87.2	872	1.6
850	63.0	862	66.1		

Table 23: Transmission data for filter 915/28 (ESO # 854)

Wavelength nm	Transmission %	Wavelength nm	Transmission %	Wavelength nm	Transmission %
876	0.27	908	89.25	940	1.97
878	0.28	910	89.34	942	1.25
880	0.35	912	91.48	944	0.75
882	0.54	914	93.69	946	0.52
884	0.66	916	94.82	948	0.35
886	0.90	918	93.49	950	0.27
888	1.50	920	89.28	952	0.19
890	2.36	922	81.52	954	0.18
892	4.15	924	70.18	956	0.18
894	7.83	926	55.65	958	0.12
896	15.59	928	40.36	960	0.04
898	31.09	930	26.74	962	0.11
900	55.11	932	16.25	964	0.06
902	78.38	934	9.68	966	0.07
904	90.44	936	5.57	968	0.10
906	91.21	938	3.30	970	0.15

Table 24: Transmission data for filter OIII/8 (ESO # 859)

Wavelength nm	Transmission %	Wavelength nm	Transmission %	Wavelength nm	Transmission %
492.00	0.15	501.00	78.52	510.00	4.06
493.00	0.28	502.00	82.21	511.00	1.94
494.00	0.54	503.00	82.62	512.00	1.01
495.00	1.10	504.00	82.66	513.00	0.56
496.00	2.44	505.00	79.81	514.00	0.33
497.00	6.04	506.00	68.17	515.00	0.20
498.00	15.55	507.00	44.13	516.00	0.13
499.00	36.77	508.00	21.15		
500.00	64.27	509.00	9.10		

Table 25: Transmission data for filter Halpha/7 (ESO # 856)

Wavelength nm	Transmission %	Wavelength nm	Transmission %	Wavelength nm	Transmission %
647	0.10	656	60.33	665	9.79
648	0.16	657	83.40	666	4.32
649	0.28	658	90.53	667	2.03
650	0.52	659	90.82	668	1.03
651	1.02	660	88.56	669	0.56
652	2.15	661	83.30	670	0.33
653	4.94	662	70.05	671	0.20
654	12.38	663	45.95	672	0.13
655	30.30	664	22.53		

A.3.3 Narrow-band Filters

TBC

Table 26: Transmission data for filter 665/12 (ESO # 858)

Wavelength nm	Transmission %	Wavelength nm	Transmission %	Wavelength nm	Transmission %
652	0.41	663	86.21	674	11.42
653	0.65	664	85.64	675	6.20
654	1.08	665	85.48	676	3.43
655	1.87	666	85.76	677	2.00
656	3.40	667	85.31	678	1.22
657	6.59	668	83.91	679	0.79
658	13.26	669	80.78	680	0.52
659	27.12	670	73.01	681	0.35
660	49.99	671	57.36	682	0.24
661	73.46	672	37.74	683	0.17
662	84.91	673	21.39	684	0.13

Table 27: Transmission data for filter SIIr/5 (ESO # 857)

Wavelength nm	Transmission %	Wavelength nm	Transmission %	Wavelength nm	Transmission %
666	0.12	674	60.14	682	2.46
667	0.22	675	79.05	683	1.16
668	0.41	676	75.53	684	0.58
669	0.85	677	61.08	685	0.31
670	1.89	678	42.77	686	0.17
671	4.58	679	24.88	687	0.10
672	11.95	680	12.24		
673	30.01	681	5.53		

A.4 Grism Transmission Curves

TBD

A.5 Grism Transmission Tables

TBD

A.6 Sample Observation Block

TBD

A.7 Photometric Standards

TBD

A.8 Polarimetric Standards

TBD

A.9 Astrometric Standard Fields

TBD

A.10 Sample FITS Headers

TBD

A.10.1 Raw Frame

TBD

A.10.2 Calibration Data*

TBD

A.10.3 Pipeline-reduced Frame*

TBD

A.11 Pointers to Sample Observations

TBD

B Subject Index

TBD